NATIONAL ADVISORY COMMITTEE FOR AERONAUTICS

REPORT 1329

FAR NOISE FIELD OF AIR JETS AND JET ENGINES

By EDMUND E. CALLAGHAN and WILLARD D. COLES

1957

For sale by the Superintendent of Documents, U. S. Government Printing Office, Washington 25, D. C. Yearly subscription, $10; foreign, $11.25; single copy price varies according to size - - - - - - - - - Price 25 cents

REPORT 1329

FAR NOISE FIELD OF AIR JETS AND JET ENGINES

By EDMUND E. CALLAGHAN and WILLARD D. COLES

Lewis Flight Propulsion Laboratory
Cleveland, Ohio

National Advisory Committee For Aeronautics

Headquarters, 1512 H Street NW., Washington 25, D. C.

Created by Act of Congress approved March 3, 1915, for the supervision and direction of the scientific study of the problems of flight (U. S. Code, title 50, sec. 151). Its membership was increased from 12 to 15 by act approved March 2, 1929, and to 17 by act approved May 25, 1948. The members are appointed by the President and serve as such without compensation.

REPORT 1329

FAR NOISE FIELD OF AIR JETS AND JET ENGINES[1]

By Edmund E. Callaghan and Willard D. Coles

SUMMARY

An experimental investigation was conducted to study and compare the acoustic radiation of air jets and jet engines. A number of different nozzle-exit shapes were studied with air jets to determine the effect of exit shape on noise generation. Circular, square, rectangular, and elliptical convergent nozzles and convergent-divergent and plug nozzles were investigated.

At low jet pressure ratios (less than 2.2) the nozzle-exit shape had a negligible effect on the sound field; at higher pressure ratios the convergent and plug nozzles exhibited discrete frequencies associated with shock waves in the jet. The convergent-divergent nozzle showed a substantial reduction in sound power at its design pressure ratio. This reduction resulted from the elimination of discrete frequencies caused by shock formations.

The acoustic power radiated by jets issuing from conical convergent nozzles was correlated by the Lighthill parameter for both air jets and nonafterburning jet engines. The ratio of sound power to Lighthill parameter was 2.7×10^{-5} for both air jets and jet engines. This result shows that the principal contribution to jet engine noise is the turbulent mixing of the jet with the surrounding medium. The sound power radiated by an afterburning jet engine was lower than indicated by the Lighthill relation.

Correction of sound-pressure-level directional data by the nozzle area ratio and the eighth power of the velocity ratio gave good agreement between engine and air-jet data.

The spectral distributions of the sound power for the engine and the air jet were in good agreement for the case where the engine data were not greatly affected by reflection or jet interference effects. Such power spectra for a subsonic or slightly choked engine or air jet show that the peaks of the spectra occur at a Strouhal number of 0.3.

INTRODUCTION

It is well recognized that the jet engine has created a formidable noise problem for operation from airports near residential communities. The promise of larger, more powerful engines in greatly increased usage has even further magnified the problem. As a consequence, the noise emanating from air jets and jet engines and means for its reduction have been under intensive study in both the United States and Great Britain. Jet engine noises can be categorized generally as (1) internal noises created inside the engine and propagated outward through the inlet and tailpipe and (2) external noises resulting from the mixing of the jet with the surrounding atmosphere. Internal noises, in general, result from flow instabilities and turbulence in the compressor, the combustors, or the turbine. An example of such noise is compressor whine.

The external noises caused by the jet are associated with two separate regimes (ref. 1), a subsonic or transonic mixing regime where no severe shock waves exist, and a supersonic overchoked regime wherein the noise results from both turbulent mixing and shock waves. The sound fields associated with these two regimes are greatly different. As might be expected, the sound field spectrum generated by a mixing process at low jet pressure ratio (less than 2.2) is more or less random in nature as is indeed the turbulence with which it is associated. At high jet pressure ratios the jet is overchoked, and the jet static pressure, after leaving the nozzle, is greater than the surrounding atmosphere and thus results in strong shock formations. In this case the sound spectra have discrete frequencies of greater amplitude imposed on the mixing noise. The sound power in these discrete frequencies is usually sufficiently high to override the turbulent mixing noise.

Reference 2 suggests that the mechanism causing the discrete frequencies in overchoked flows depends on a regular stream disturbance traversing the shock pattern in the jet. This action is of a self-propagating nature, as described in reference 2, and the frequency of the emission depends on the diameter of the jet and the spacing of the shock waves. It would appear therefore that changes in nozzle shape would alter such a sound generation mechanism. In fact, by proper design of either convergent-divergent or plug nozzles, high-pressure-ratio operation should be possible without shock waves and hence discrete frequencies.

Fortunately, with respect to the jet aircraft takeoff noise problem, the nozzle or engine pressure ratios of current and contemplated turbojet engines are not sufficiently high to produce severe shock waves at static sea-level and takeoff thrust conditions. There may, however, be flight noise problems involving either aircraft structure or passenger comfort arising at the high nozzle pressure ratios associated with high forward speeds.

It is obvious that a fundamental first step in the understanding of jet engine noise is to establish the relation between the internal and external noises at takeoff, that is, at essentially static thrust conditions. If the noise generation of a simple air jet, properly extrapolated, is compared to that of a jet engine, it should be possible to determine the contributions of both external and internal engine noise.

[1] Supersedes NACA TN 3590, "Investigation of Far Noise Field of Jets, I—Effect of Nozzle Shape," by Edmund E. Callaghan and Willard D. Coles, 1955, and NACA TN 3591, "Investigation of Far Noise Field of Jets, II—Comparison of Air Jets and Jet Engines," by Willard D. Coles and Edmund E. Callaghan, 1955.

Fortunately a method for correlating the mixing noise from subsonic air jets is presently available. The general theory of noise created aerodynamically (turbulent-mixing noise) was proposed by Lighthill (ref. 3). Lighthill analyzed theoretically the sound field resulting from a region of turbulence located in a uniform acoustic medium. Application of this theory predicts the variation of the sound-power generation with conditions of the jet and the surrounding medium but does not predict the magnitude of the sound-power generation. Experimental evidence to date supports this result (refs. 4 and 5).

The investigation reported herein was conducted to determine (1) the relation between internal and external noise created by a jet engine and (2) the effect of nozzle shape on the noise created by turbulent mixing and shock waves. Noise generation by several jet engines and a series of small (area approx. equivalent to 4-in.-diam. circular nozzle) nozzles of various shapes was studied. The small-scale nozzles used were both low-pressure-ratio-design convergent nozzles (circular, square, rectangular, and elliptical exits) and high-pressure-ratio-design nozzles (convergent-divergent and plug nozzles designed for shock-free expansion of the jet to supersonic velocities). These tests were conducted at the NACA Lewis laboratory and represent a portion of a study of jet noise and means for its suppression.

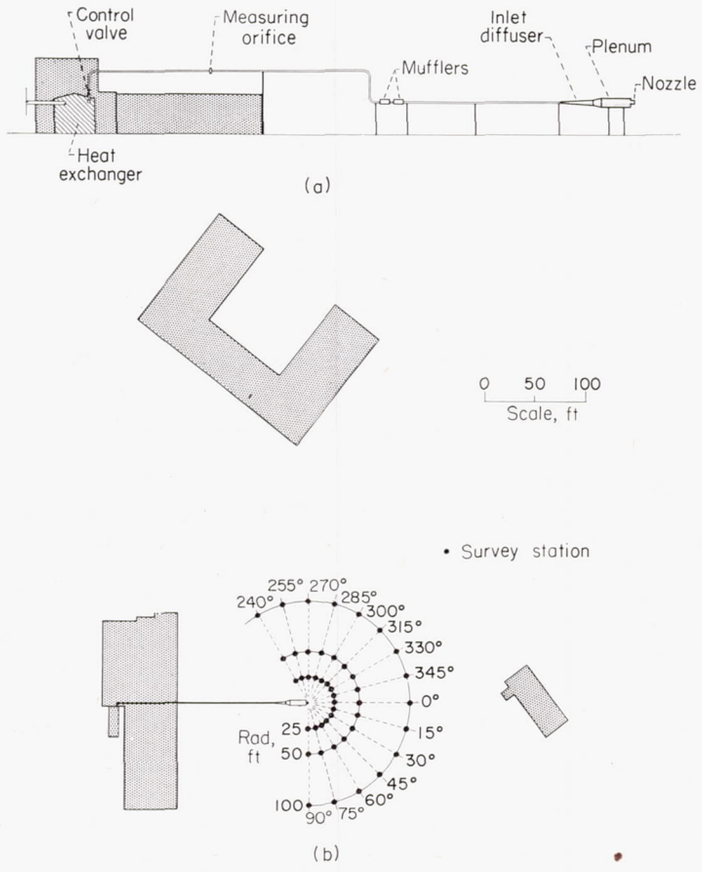

(a) Elevation; side view.
(b) Plan view.

FIGURE 1.—Schematic diagram of air system and adjacent buildings.

APPARATUS AND PROCEDURE

AIR JET

A schematic diagram showing the piping layout for the air supply to the air jet is shown in figure 1. Air is supplied at a pressure of either 40 or 125 pounds per square inch gage from compressors situated at a considerable distance from the experimental setup. Moisture separation equipment is included in the air supply system; but to eliminate condensation effects at the nozzles, the air was heated to approximately 200° F in the large gas-fired heat exchanger (fig. 1). The air jet was located to provide a sound field free of buildings and other reflecting surfaces. The nearest reflecting surface downstream of the air jet was a low building 190 feet distant. At the sides, the nearest building was 230 feet away, and the building housing the control room and heat exchanger was 125 feet upstream of the air jet. A photograph of the plenum chamber with a nozzle installed is shown in figure 2.

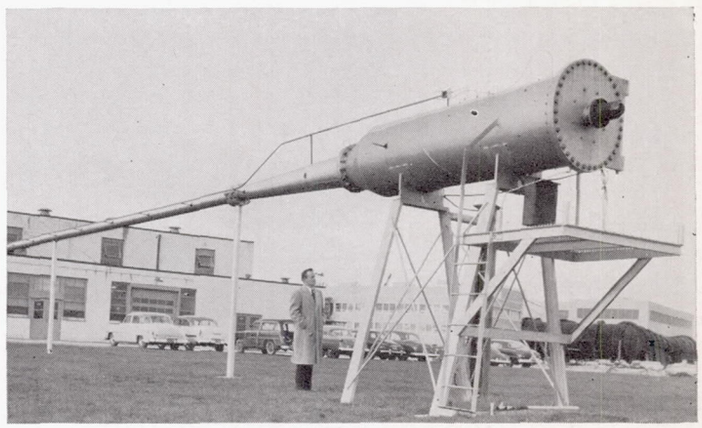

FIGURE 2.—Nozzle, plenum chamber, and associated piping.

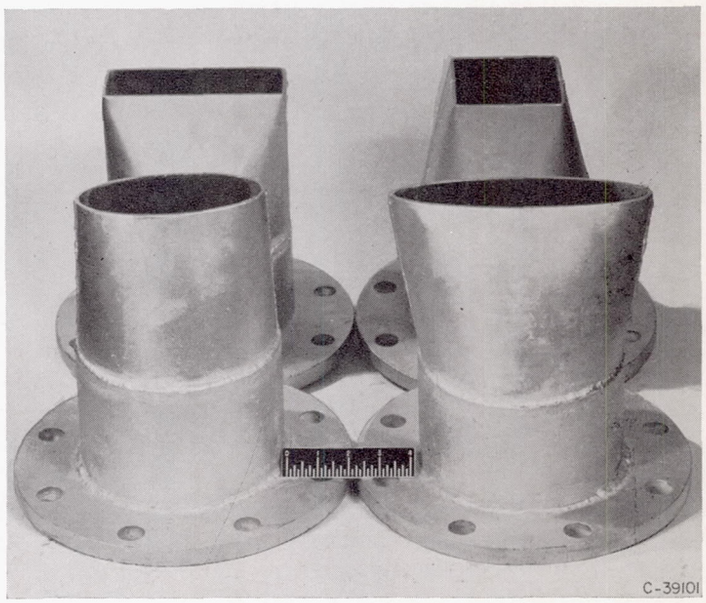

FIGURE 3.—Square, rectangular, and elliptical convergent nozzles.

In order to ensure that the generation of the extraneous noise from the piping and associated equipment would be kept to a minimum, the following precautions were taken:

(1) The pressure control valve was of a design having low-noise-level characteristics and was located inside the building approximately 175 feet from the air jet.

(2) The flow-measuring orifice was located approximately 150 feet from the jet.

(3) Two mufflers were provided downstream of the last bend in the line.

(4) A diffuser section equipped with screens was used to prevent flow separation and provide a uniform velocity profile at the plenum inlet.

(5) The large plenum was used to provide low air velocity upstream of the nozzle.

(6) A smooth bellmouth entry to the nozzles was provided.

The total pressure and temperature of the air were measured at the plenum chamber. In general, the controls used on the throttling valve and the air heater kept pressure and temperature deviations within ± 0.1 inch of mercury and $\pm 10°$ F, respectively, of the prescribed setting.

Seven convergent nozzles, a convergent-divergent nozzle, and two types of plug nozzles were investigated. Three of the convergent nozzles were 60° conical nozzles with 3-, 4-, and 5-inch-diameter throats. The other convergent nozzles had square, rectangular, and elliptical cross sections (fig. 3) and had throat areas equal to that of the 4-inch-diameter conical nozzle. The two elliptical nozzles had axis ratios of 2 and 4. The convergent-divergent nozzle (fig. 4(a)) had a 4-inch-diameter throat and a design pressure ratio of 3.0. Two types of plug nozzles are shown in figures 4(b) to (e).

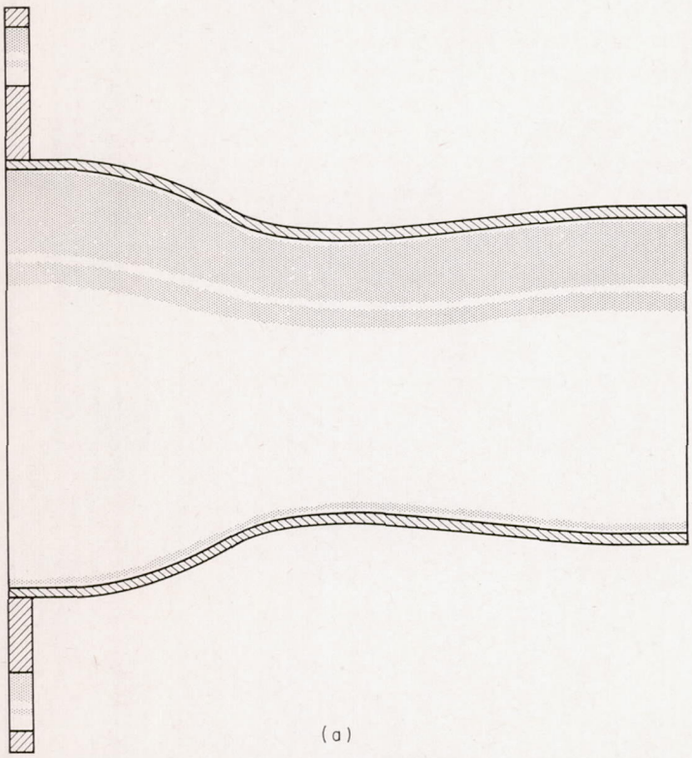

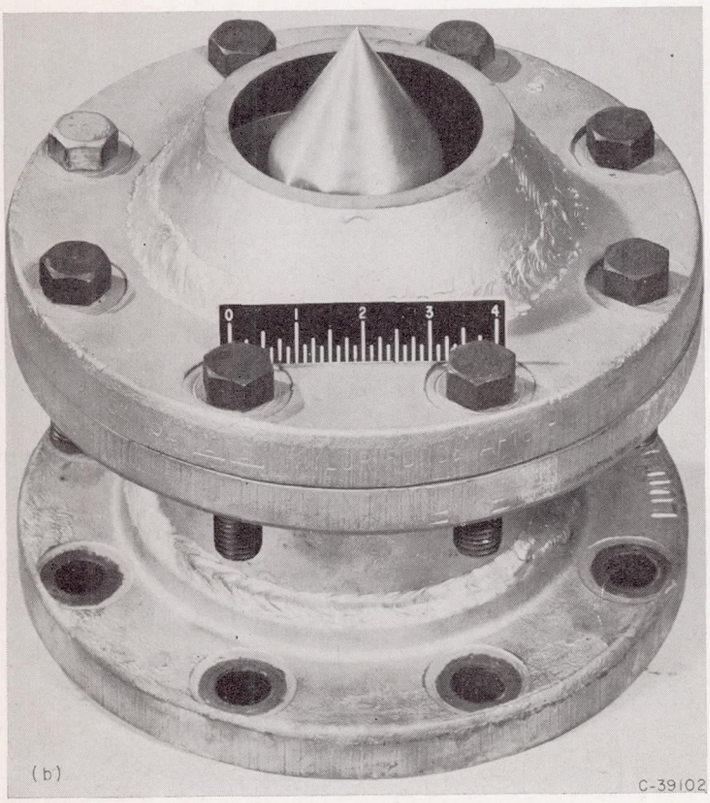

(a) Convergent-divergent nozzle; design pressure ratio, 3.0; 4-inch-diameter throat.

(b) Conical plug; design pressure ratio, 4.0.

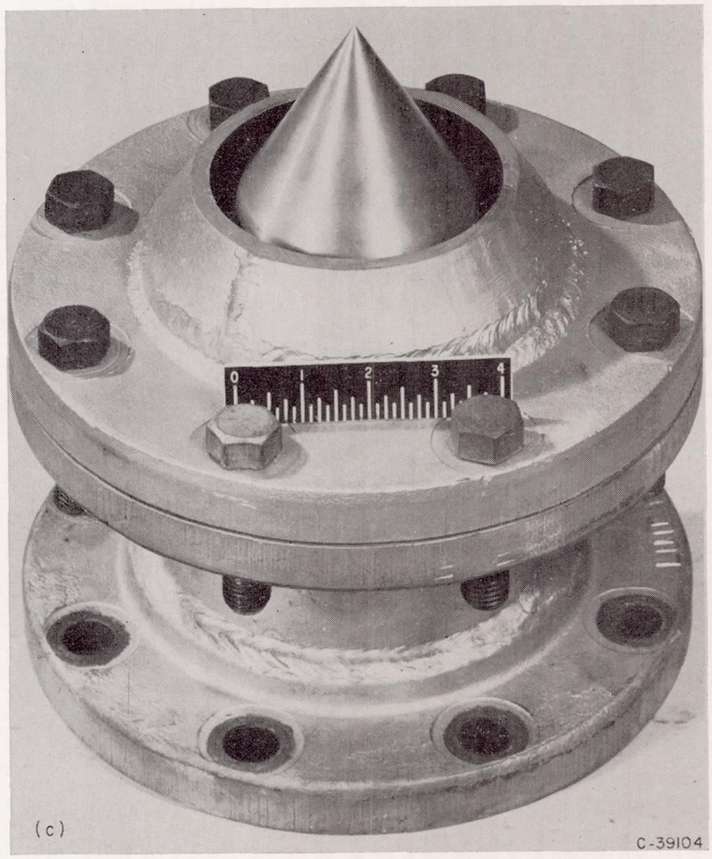

(c) Conical plug; design pressure ratio, 9.5.

FIGURE 4.—Nozzles designed for high pressure ratios.

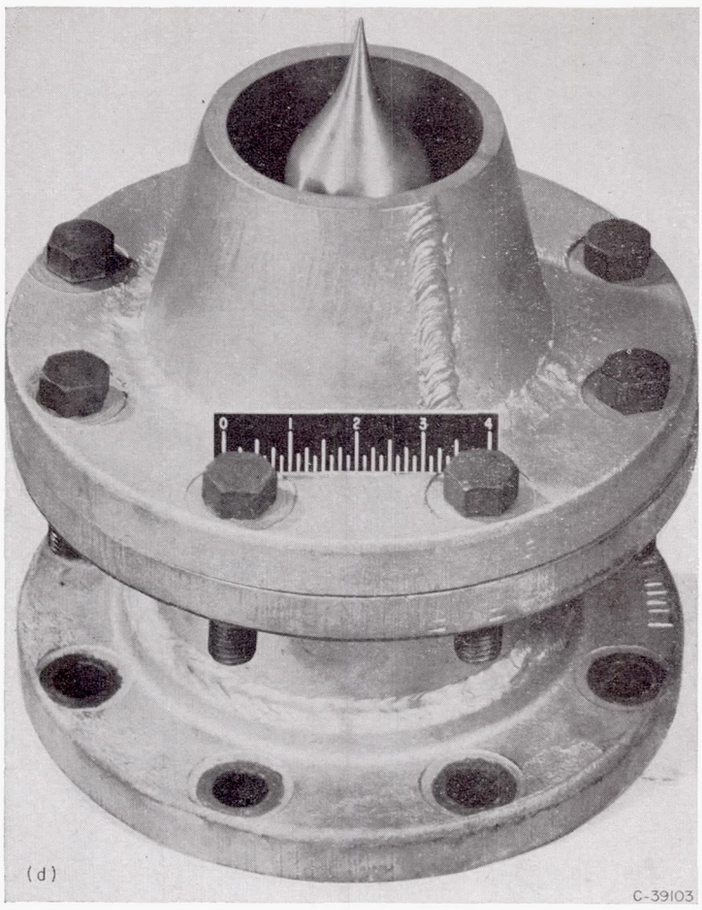

(d) Isentropic plug; design pressure ratio, 4.0.

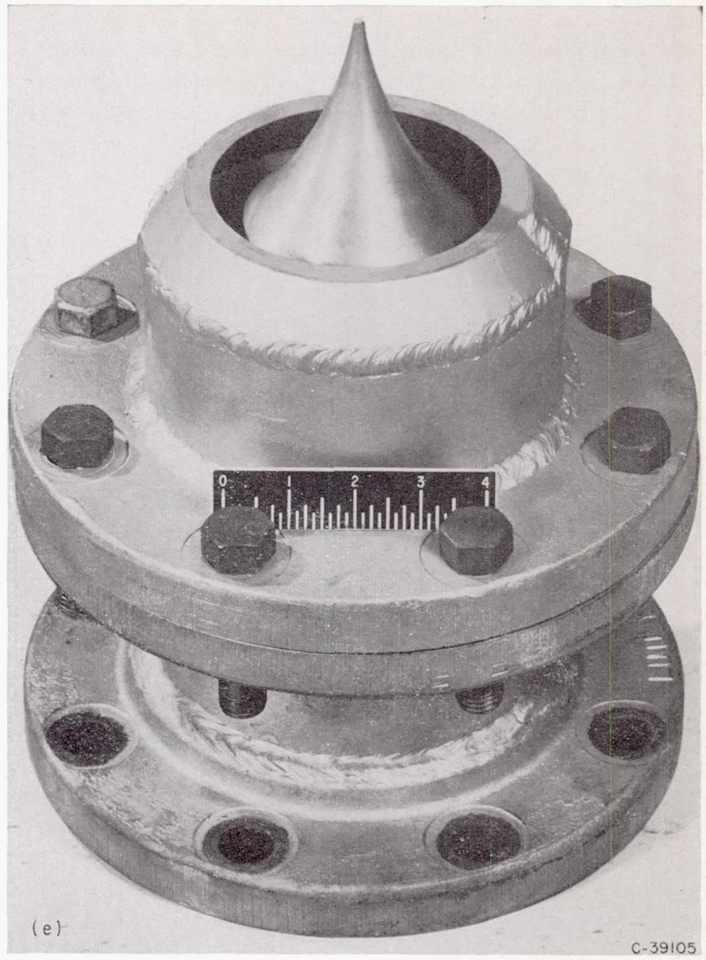

(e) Isentropic plug; design pressure ratio, 9.5.

FIGURE 4.—Concluded. Nozzles designed for high pressure ratios.

One type had conical plugs, and the other type had plugs giving approximately isentropic expansion of the jet. Nozzles of each type having design pressure ratios of 4.0 and 9.5 were used.

The following procedure was used with each nozzle configuration. Air-jet pressure conditions were established in pressure increments of 4 inches of mercury, in ascending order, since preliminary tests showed no effect of ascending or descending pressures. Sound-level surveys were made at each value of jet total pressure over a range of plenum-chamber- to ambient-pressure ratio from approximately 1.45 to 3.25 for the low-pressure-design nozzles and 1.45 to 4.2 for the high-pressure-design nozzles.

TURBOJET ENGINES

The turbojet engines used in the investigation were of the axial-flow type and had rated sea-level thrust values of 5000, 10,000, and 8700 pounds; they are hereinafter referred to as engines A, B, and C. Under rated conditions, the total- to static-pressure ratio across the exhaust nozzle was 1.7 for the smaller engine (engine A) and approximately 2.2 for the larger engines (engines B and C). Each of the engines was mounted in the thrust stand, which is shown with engine B in figure 5. The engines were equipped with large inlet bellmouth sections, and a screen was provided at the bellmouth entrance to prevent ingestion of foreign material.

In addition to thrust, fuel and air flows through the engine and jet temperature were measured in order to check engine performance and determine jet velocity, which is of prime importance in the aerodynamic generation of sound.

Engine A was tested at two elevations above the ground, first with the engine centerline 6 feet above the ground and later with the engine centerline 8 feet above the ground. Engines B and C were mounted 6 and 8 feet above the ground, respectively. All the engines were equipped with convergent exhaust nozzles.

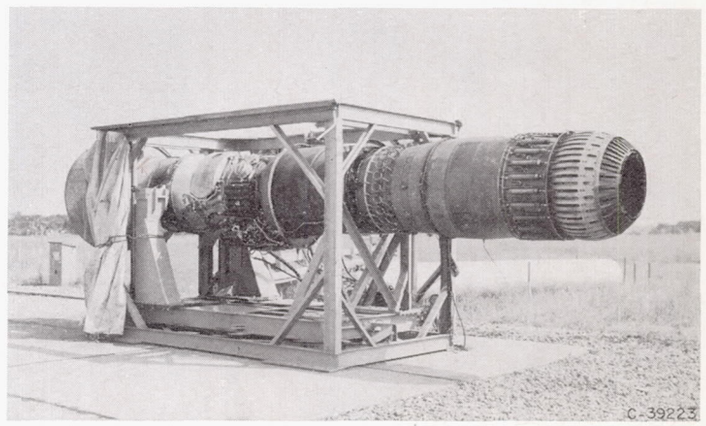

FIGURE 5.—Thrust stand with engine B installed.

ACOUSTIC MEASUREMENTS

For purposes of standardization of nomenclature, the acoustic terms used herein are those defined in reference 6. Sound-pressure-level measurements were made with a commercial sound-level meter set to a flat response. Frequency distributions were measured with an automatic audio-frequency analyzer and recorder having a frequency range from 35 to 18,000 cycles per second. This range is divided into 27 bands of ⅓-octave width. Before each test, both the analyzer and sound-level-meter systems were calibrated with a small loudspeaker-type calibrator and transistor oscillator. The frequency analyzer was mounted in an acoustically insulated panel truck.

Air jet.—Sound measurements were taken at radial distances of 25, 50, and 100 feet from the jet (fig. 1). Measuring stations were located at 15° increments of azimuth over the range from 120° from the jet axis on one side to 90° from the jet axis on the other. The plenum chamber and nozzle assembly were 10 feet above the ground plane, and all the sound measurements, except the frequency measurement, were made at that height. The frequency distribution data were made approximately 6 feet above ground level at a distance of 50 feet. Spectra were obtained at 30° and 90° azimuths (fig. 1) for all the nozzles at each pressure ratio. A complete spectrum survey (all azimuths) was made at several pressure ratios using the 4-inch-diameter convergent nozzle.

A small error in the total acoustic power resulted because no sound-pressure measurements were made upstream of 120° from the jet axis. This error was quite small, since the sound-pressure levels in this area were always 10 decibels or more below the maximum value and contributed very little to the total acoustic power.

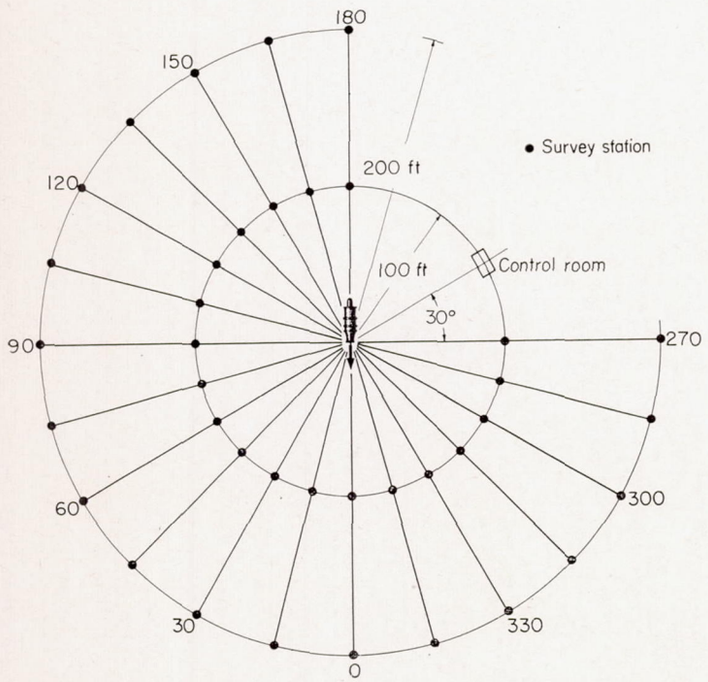

FIGURE 6.—Location of engine sound survey stations and control room.

Although extreme care was taken to calibrate the sound-measuring equipment, other sources of error affected the results. Because the jets were small, the wind had a considerable effect on the jet direction. No tests were made at wind velocities greater than 10 miles per hour, but some errors did occur because of wind gusts. Tests made on different days with the same nozzle showed that local sound-pressure-level variations might be as high as ±3 decibels. However, the sound-power levels always varied less than ±1 decibel. The sound power should be expected to have less error, since it results from an integration over the whole sound field, and errors in local values would tend to average out.

Engines.—Figure 6 shows the plan view of the engine sound field. The over-all sound measurements were taken 4 to 5 feet above ground level for cases where the engine centerline height was 6 feet above the ground and at engine centerline height when the engine was mounted 8 feet above the ground. Sound measurements were taken in 15° increments for engine A at both 100- and 200-foot radii from the engine, and for engines B and C at 200-foot radii. The control room was located about 100 feet from the engine in the quadrant in which no sound measurements were taken and, because of its small size and location, had negligible sound-reflection effects. The nearest large reflecting surface forward of the engine was approximately 500 feet away, and the sound field to the rear and sides was unobstructed for over ½ mile.

Measurements were usually taken at each of the sound measurement stations at one or more radial distances for the air jet (fig. 1(b)) and the engines (fig. 6). Frequency spectra were measured when the over-all field survey was made, but at one radial distance (nonafterburning engine, 200-ft rad.; afterburning engine, 400-ft rad.). The microphone was located 6 feet above the ground for all cases.

Spectra were obtained at all azimuths between 15° and 180° (fig. 6) for each of the engines over a range of engine power conditions.

RESULTS AND DISCUSSION

To define any noise source, it is necessary to know the total sound power radiated, its frequency spectrum, and its directionality pattern. Comparisons of various sources must be based on all three factors. Changes in either directionality pattern or frequency spectrum which lower peak values could greatly alleviate the noise problems of current engines.

TOTAL ACOUSTIC POWER

The total acoustic power radiated by a jet can be calculated from the measured sound-pressure levels by the procedure described in reference 7. The essential assumptions for these calculations are as follows: symmetry of the sound field about the jet axis, a ground plane acting as a perfect reflector, and a sufficiently large distance from the effective source to the observer, that is, the sound waves are essentially plane waves. Many of the sound-power data contained herein are presented in watts. For convenience, reference is also occasionally made to sound power in decibels (based on a reference power of 1×10^{-13} watts).

Circular convergent nozzles with air jet.—The sound power radiated by circular convergent nozzles (3-, 4-, and 5-in. diam.) as a function of jet pressure ratio is shown in figure 7. (The jet pressure ratio, as used in this report, is the ratio of the plenum-chamber total pressure to the atmospheric pressure.) As expected, there are separate curves for each nozzle diameter. Data at high pressure ratio for the 5-inch-diameter nozzle were not taken because of air-supply limitations. Figure 7 shows at least two distinctly different curves for each nozzle, which depend on the pressure ratio. Above a pressure ratio of 2.1, there is a distinct increase in the sound power with pressure ratio. This increase in the rate of sound output results from shock-wave formations in the jet (ref. 2). At pressure ratios above 2.6, the curves show a tendency to flatten up to a pressure ratio of about 2.9, above which the sound power for the 3-inch-diameter jet again shows a marked tendency to increase. The other nozzles might also have shown similar increases at the higher pressure ratios.

Lighthill predicted a linear variation of radiated sound power with jet nozzle area (ref. 3). This prediction is verified in figure 8, a plot of the ratio of total sound power to nozzle area as a function of jet pressure ratio for the three circular nozzles. Although Lighthill's theory only applies to pressure ratios less than choking (1.89), the data for the three nozzles fall along a single curve for the whole range of pressure ratios investigated. The data for figures 7 and 8 at pressure ratios less than 1.89 are shown in figure 9 in terms of the Lighthill sound-generation parameter

$$\rho_0 A V^8 / a_0^5$$

where

ρ_0	ambient air density, slugs/cu ft
A	nozzle-exit area, sq ft
V	jet velocity, ft/sec
a_0	ambient acoustic velocity, ft/sec

In figure 9 the total sound power is plotted as a function of the Lighthill parameter, both in watts. The good correlation is expected from the good subsonic correlation of figure 8. The Lighthill parameter and pressure ratio are directly related for these tests, since the atmospheric conditions and jet total temperature are essentially constant. Hence, ρ_0 and a_0 are nearly constant. Since V is related directly to pressure ratio at constant total temperature, the good correlation of figure 9 follows naturally from figure 8. In addition, a line of unity slope (fig. 9) drawn through the data points verifies the prediction of Lighthill. It is interesting to note that the free-field measurements of figure 9 agree well with the reverberant-chamber data of reference 4.

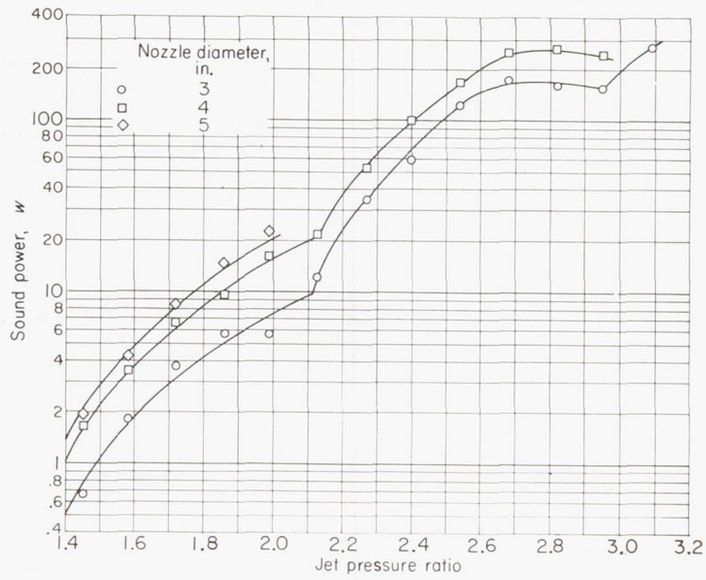

FIGURE 7.—Sound power as function of jet pressure ratio for three circular convergent nozzles.

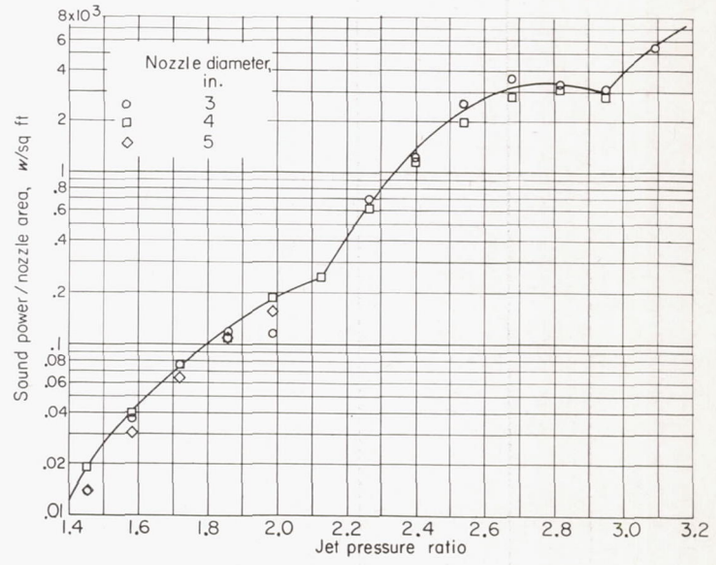

FIGURE 8.—Sound power per unit nozzle area as function of jet pressure ratio for circular convergent nozzles.

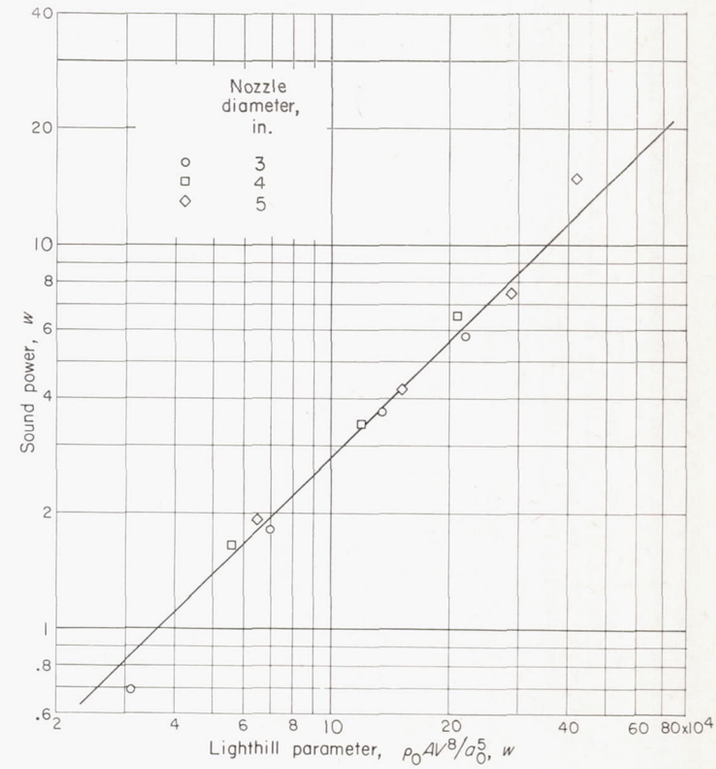

FIGURE 9.—Sound power as function of Lighthill parameter (ref. 3) for three circular convergent nozzles. Pressure ratio, less than 1.89.

Comparison of air jet and engine with circular convergent nozzles.—The data of figure 9 represent noise of purely aerodynamic origin, that is, turbulent mixing noise. If such data are extrapolated to values of the Lighthill parameter comparable to those encountered in jet engines, then it should be possible to determine what portion of the engine noise is internal and what portion external. It would appear that the only difficulty in such an extrapolation is the great temperature difference between a relatively cold air jet and a jet engine. The results of reference 8 show that at a single point in the sound field (1-in. air jet, 17° azimuth, 12.5 diam. from exit) the sound-pressure level was independent of temperature for a range of jet temperatures from 76° to 1200° F. These data are not entirely conclusive, however, since the jet was heated by direct combustion. Unpublished data using a $\frac{9}{16}$-inch air jet, heated by a heat exchanger, show no effect of jet temperature on sound-power generation for a range of jet total temperatures from 70° to 1200° F.

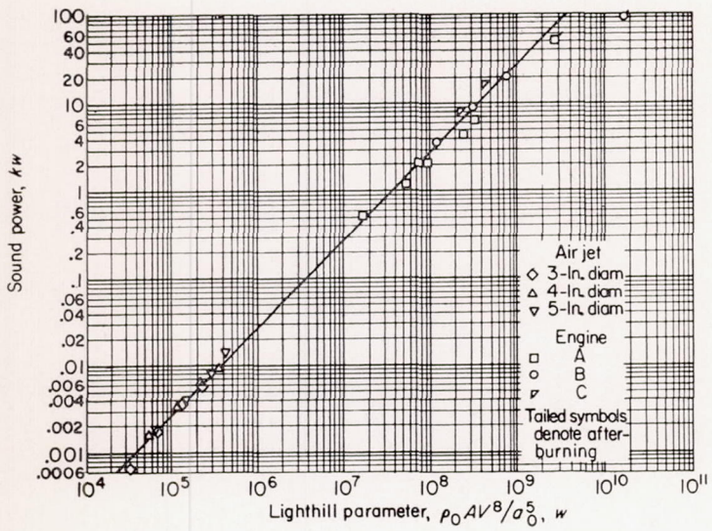

FIGURE 10.—Sound power as function of Lighthill parameter.

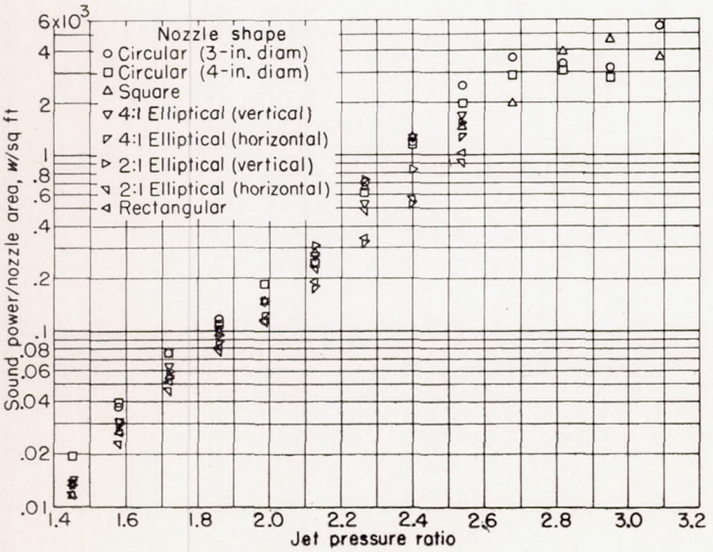

FIGURE 11.—Effect of nozzle shape on sound-power generation.

To calculate the Lighthill parameter for an engine, it is necessary to know jet velocity quite accurately. This results in several problems. At low engine thrusts the velocity profile across the exit is not uniform. At high engine thrusts the velocity profile across the exit is uniform, but if the exit is choked, the gas expands externally to a somewhat higher velocity than at the exit. It would appear that the best velocity to use would be a bulk velocity which also would reflect the external expansion of the gases to a velocity higher than at the exit at above choking conditions. The ratio of thrust to mass flow provides such an average velocity and has been used in the calculation of the Lighthill parameter for the engine.

Figure 10 shows the total sound power in kilowatts for both the air jet and engines as a function of the Lighthill parameter. The engine data are presented for operation with and without afterburning. The air-jet data for three nozzle sizes at pressure ratios below that for choked flow are those of figure 9. The line on figure 10 represents the best line through the data excluding the afterburning data. The fact that the slope of the line is exactly unity shows that, although the engine jet temperature is high and the flow slightly supersonic for the high-thrust condition of engines B and C, the sound power is well represented by the Lighthill parameter. These results show that the ratio of sound power to Lighthill parameter is 2.7×10^{-5}.

This correlation shows that, basically, the noise generated by a full-scale engine is governed by the same law as the noise of a simple air jet. Hence, it may be concluded that the principal contribution to jet engine noise arises from the turbulent mixing of the jet with the surrounding atmosphere.

There is some scatter of the data, as might be expected, since the probable accuracy of the results is ± 1 decibel. There are no definable trends which might be attributed to any particular difference such as changes in engine height above ground. It is probable that the scatter is caused by the wide range of ambient test conditions encountered between winter and summer.

The afterburner data for both engines fall somewhat below the straight-line relation indicated for the other data. There are two probable explanations for this effect: (1) The high-temperature afterburning condition is beyond the limits of applicability of the Lighthill parameter, without considering jet density; or (2) the sound pressures generated by an afterburning jet may be of such large magnitude that the radiated sound waves are no longer of small amplitude and hence would be subject to the large attenuation effects associated with finite waves (ref. 9).

Effect of nozzle shape of convergent nozzles with air jet.—The effect of nozzle shape on the sound power generated is shown in figure 11 as a plot of sound-power to nozzle-area ratio as a function of jet pressure ratio for the circular (3- and 4-in. diam.), square, rectangular, and elliptical nozzle-exit shapes. In general, nozzle-exit shape does not have much effect on sound-power generation. The spread in the data for pressure ratios less than 2.2 amounts to only a 3-decibel variation in sound power. There is a tendency for most of the data to fall below those for the circular nozzle. This is

438639—58——2

particularly true for the pressure ratios between choking (1.89) and 2.6 and is believed to result from the asymmetric nozzle shapes, which would alleviate the discrete-frequency sound generation described in reference 5.

It should be noted that the sound power (when calculated by the method of ref. 7) is slightly different for the horizontal and vertical orientations of both elliptical nozzles. Since the calculated powers are slightly different for the same nozzle in two different orientations, it is obvious that the sound field is not rotationally symmetrical as assumed. The actual sound power would therefore lie approximately midway between the points for vertical and horizontal positions of the nozzle. Since the entire spread for all nozzles is small, this would not appear to be an important effect. For axis ratios greater than 4 to 1, however, such effects may be considerably greater.

Convergent-divergent and plug nozzles with air jet.—Shock waves in the jet materially increase the sound power radiated by the jet. The convergent-divergent and plug-type nozzles used in this investigation were designed to provide shock-free flow at a particular pressure ratio. The design pressure ratio of the convergent-divergent nozzle was 3.0. Figure 12 shows the sound-power to nozzle-area ratio as a function of pressure ratio for this nozzle. Also shown in the figure are the convergent-nozzle data of figure 8 and a curve corresponding to a V^8 relation of sound power to velocity. For this curve, the velocity was calculated for fully expanded isentropic flow from the pressure ratio and jet total temperature (200° F). The data for the convergent-divergent nozzle fall slightly below the convergent-nozzle curve at the low pressure ratios, because the exit velocity from a convergent-divergent nozzle is lower than that for a convergent nozzle at any plenum-chamber total- to atmospheric-pressure ratio less than 1.87. For this particular nozzle, the throat diameter was 4.0 inches and the exit diameter 4.12 inches. For this geometry, the throat chokes at a plenum total- to atmospheric-pressure ratio of 1.46, and the flow downstream of the throat diffuses to a lower exit velocity than for the convergent nozzle.

The data for the convergent-divergent nozzle cross the V^8 curve at a pressure ratio of about 2.05 and continue upward until a sound-power peak is obtained at a pressure ratio near 2.6 (fig. 12). As the pressure ratio is increased, the sound power decreases to a minimum at a pressure ratio of 2.9. Although the general trends in the data for the convergent and convergent-divergent nozzles are somewhat similar, the decrease in sound pressure at a pressure ratio near 2.9 is much more marked for the convergent-divergent nozzle, and the sound power radiated is only one-third to one-half as much. The sound-power decrease from a pressure ratio of 2.4 to a minimum at 2.9 is of considerable interest. Decreasing the shock strength results in substantial decreases in the sound-power generation. The minimum occurs at 2.9 rather than at the design value of 3.0, because the boundary-layer buildup inside the nozzle reduces the effective area of the exit.

Figure 13 shows the sound-power to exit-area ratio as a function of jet pressure ratio for all the plug nozzles investigated. Also shown on the figure is the V^8 curve of figure 12. Neither of the nozzles with a design pressure ratio of 4.0 shows any real tendency toward decreased sound power at or near design pressure ratio, as was shown for the convergent-divergent nozzle (fig. 12). The nozzles with a design pressure ratio of 9.5 follow closely the data for the nozzles with a design pressure ratio of 4.0 over the whole range of pressure ratios investigated, with the exception of a sharply decreased sound power which occurred near a pressure ratio of 3.2 for the isentropic (9.5-pressure-ratio) plug nozzle. This decrease resulted from sudden cessation of the usual resonance or squeal associated with nozzle operation at high pressure ratios. The reasons for the decrease were not investigated with flow-visualization equipment, but they would probably become apparent from such a study. None of the nozzles showed the consistent trend toward lower noise levels evidenced by the convergent-divergent nozzle (fig. 12).

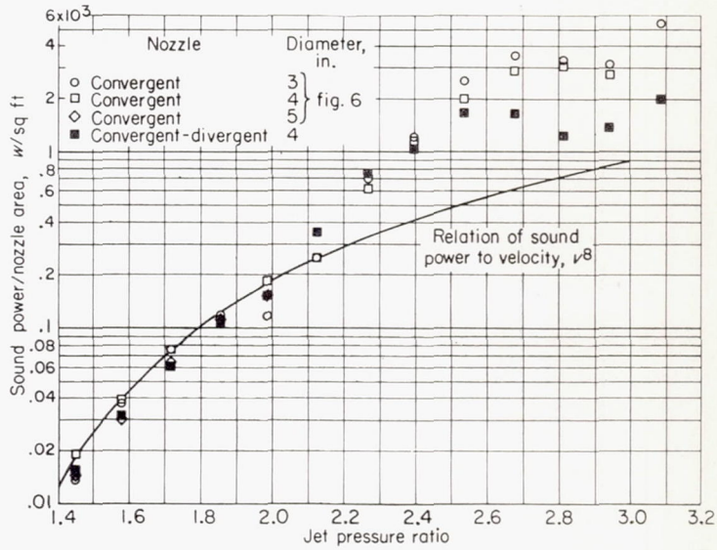

FIGURE 12.—Comparison of sound power generated by jets discharging from convergent and convergent-divergent nozzles.

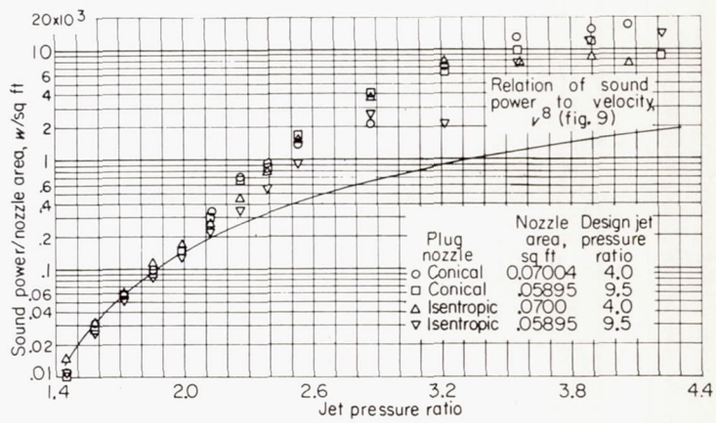

FIGURE 13.—Comparison of sound power generated by jets discharging from plug nozzles.

SOUND SPECTRA

Circular convergent nozzles with air jet.—The sound spectra of the 3-inch-diameter nozzle at a 50-foot radius and azimuths of 30° and 90° are shown in figure 14 for a wide range of pressure ratios. At both the 30° and 90° positions there is considerable similarity in the general shape of the spectra at the low pressure ratios (less than 2.2). At the higher pressure ratios the spectra show sharp peaks indicative of resonance-type noises. This is particularly evident at the 90° position. At a pressure ratio of 2.55 there is a sharp peak at 4000 cps, and at a pressure ratio of 4.15 peaks occur at 1600 and 3200 cps.

The effect of nozzle diameter on the sound spectra is shown in figure 15. As would be expected, the spectrum level increases with increasing diameter (fig. 15(a)). However, there is also a tendency for the energy to shift to higher frequencies with decreasing diameter. This is clearly illustrated in figure 15(b), a plot of the cumulative sound intensity (total intensity below a given frequency) as a function of frequency. These results are typical of all the circular-nozzle data, regardless of pressure ratio or measuring position.

The spectrum distribution of the total sound power radiated by the 4-inch-diameter circular nozzle at pressure ratios of 1.85 and 2.55 is shown in figure 16. These results were calculated from spectrum measurements made at all the 50-foot-radius positions. The sound pressures in each ⅓-octave band were integrated in the same manner as the

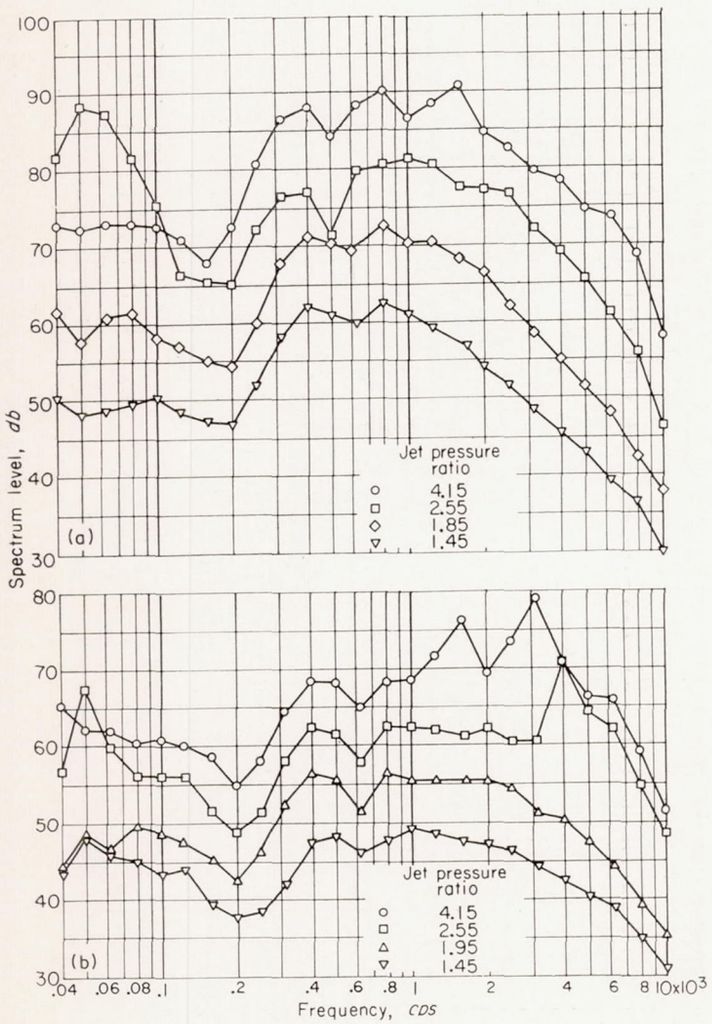

(a) Azimuth, 30°.
(b) Azimuth, 90°.

FIGURE 14.—Sound spectra of jet discharging from 3-inch-diameter convergent nozzle. Distance from jet exit, 50 feet.

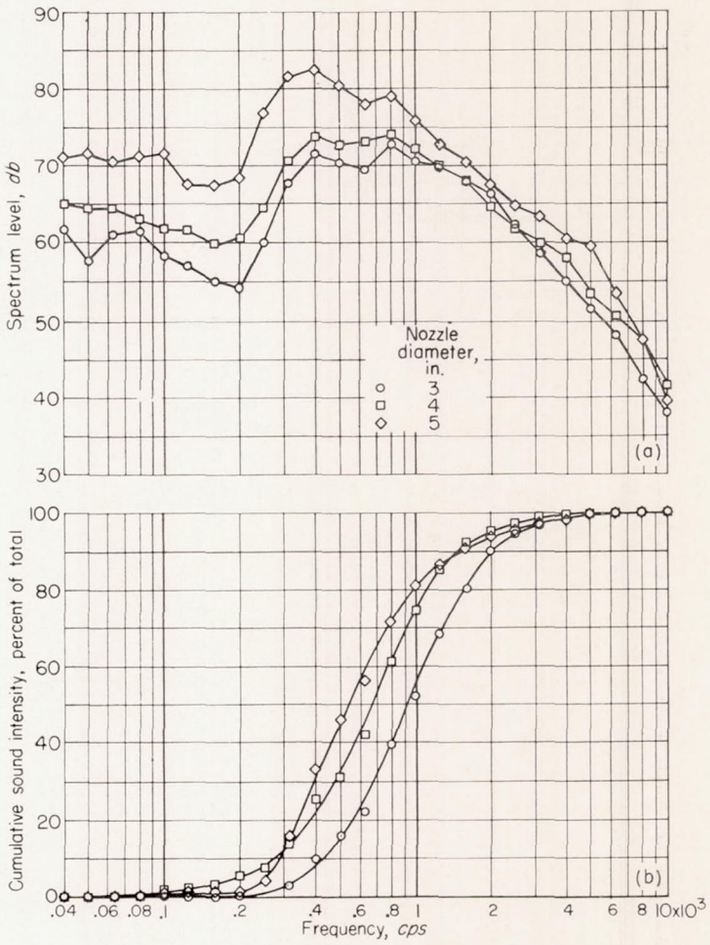

(a) Difference in level with diameter.
(b) Frequency shift with nozzle diameter.

FIGURE 15.—Effect of convergent nozzle diameter on sound spectra. Jet pressure ratio, 1.85; azimuth, 30°.

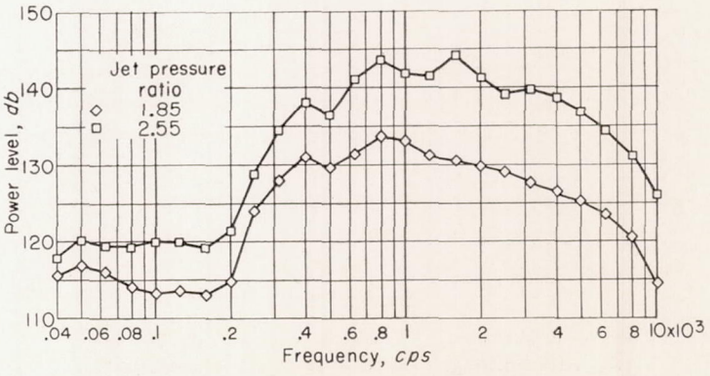

FIGURE 16.—Sound-power spectra of jet discharging from 4-inch-diameter circular convergent nozzle at several pressure ratios.

over-all sound pressures (to obtain total sound power). Sound energy increases quite rapidly above 200 cps (fig. 16). At the higher pressure ratio, a small peak in the frequency-distribution curve occurs at 1600 cps and undoubtedly results from shock formations in the jet. The cumulative sound power (total sound power below a given frequency) for these data is shown in figure 17. Less than 2 percent of the sound energy lies below 200 cps, and more than 90 percent of the sound energy lies between 200 and 4000 cps. The rather wide spread frequently encountered in the spectral data at the low frequencies results from wind noise. Data below 200 cps are greatly affected by the wind; but, since less than 2 percent of the total energy in the entire spectrum lies below 200 cps, this is not important.

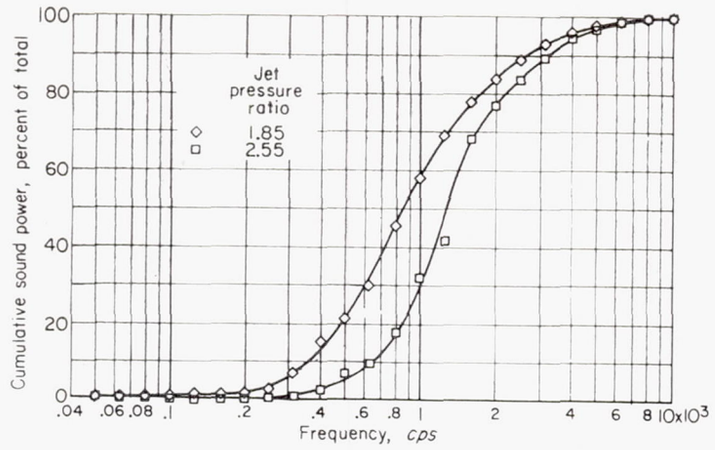

FIGURE 17.—Cumulative sound power of jet discharging from 4-inch-diameter circular convergent nozzle at several pressure ratios.

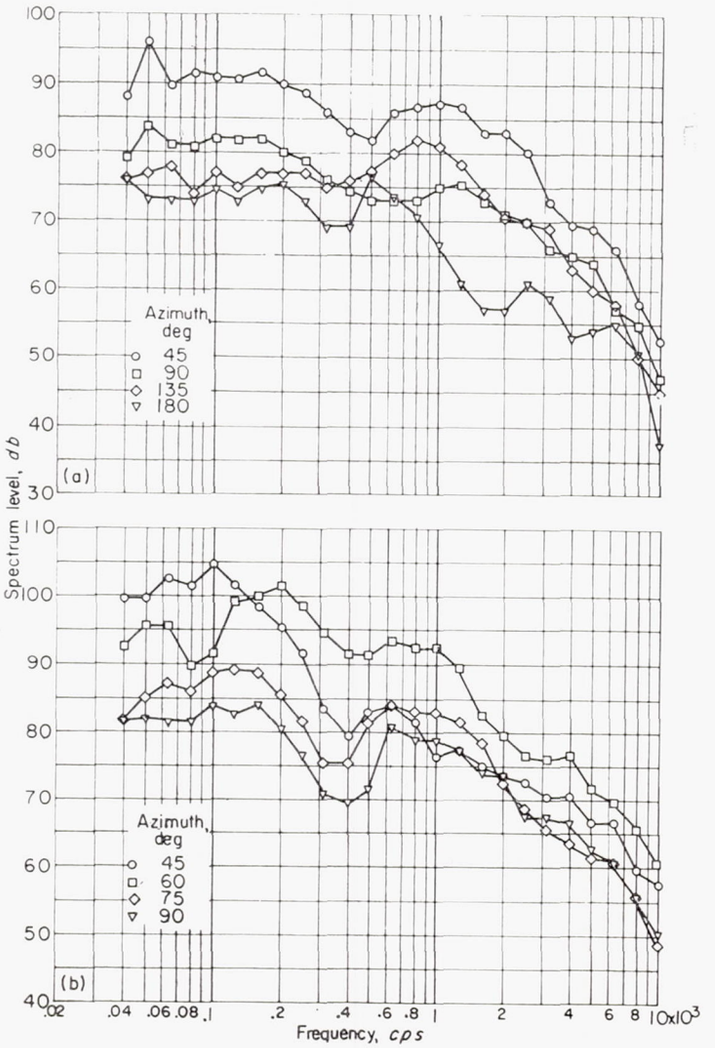

(a) No afterburning. Distance from jet exit, 200 feet.
(b) Afterburning. Distance from jet exit, 400 feet.

FIGURE 18.—Spectral distribution of noise from engine B at several azimuths.

Circular convergent nozzles with engines.—Spectrum-level distributions for engine B at four azimuths are shown in figure 18 for both afterburning and nonafterburning conditions. In general, these data show a characteristic dip in the spectra at around 400 cps with a secondary peak at around 1000 cps. The data obtained with engine C showed quite similar characteristics. With engine A, however, the measured spectrum was dependent on engine height above

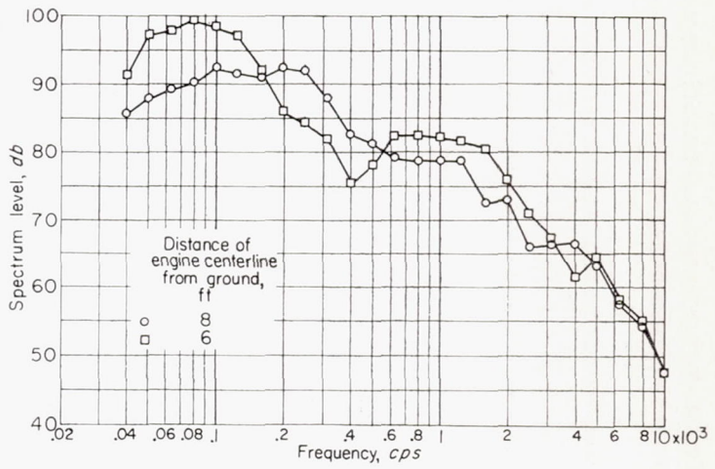

FIGURE 19.—Sound spectra for engine A for two engine elevations at 30° azimuth and distance of 200 feet.

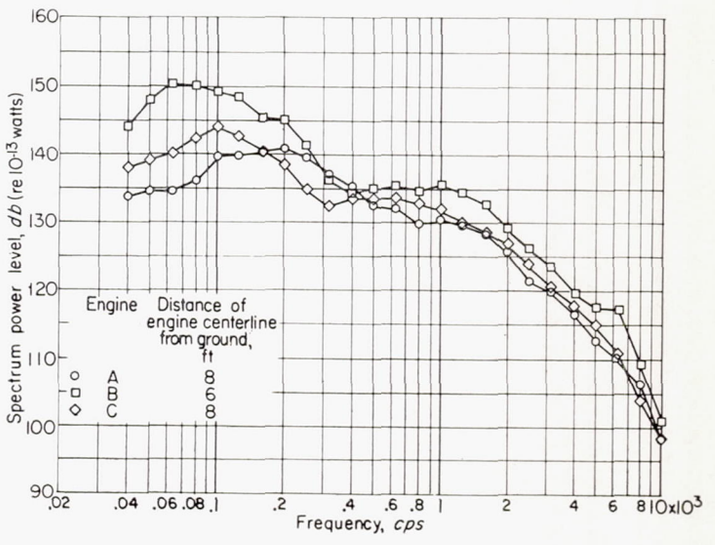

FIGURE 20.—Spectrum power level for engines A, B, and C at rated engine power conditions.

the ground. Data with this engine 6 feet above the ground were quite similar to those for engine B (fig. 18(a)); at 8 feet above ground, however, the characteristic dip and secondary peak were greatly diminished. Typical spectra for the two engine heights at the 30° azimuth are shown in figure 19. The effect of engine height on the spectra undoubtedly results from ground interference or reflection effects (ref. 10). The results of reference 10 indicate that reflection causes just such characteristic dips and peaks in the spectra and that increasing source and receiver height diminish the effect. Furthermore, the band width of the analyzer has a strong effect on the results, and a relatively narrow band instrument (⅓-octave) shows these effects more clearly than a wider band analyzer.

Figure 20 shows the spectrum power level (total radiated sound power per cycle) as a function of frequency for all three engines at rated engine conditions. The characteristic spectrum dip and peak previously discussed also show up on these data. Engine B data show this effect to the greatest extent, engine C data somewhat less, and engine A data only a little. This lends considerable credence to the hypothesis that reflection effects cause these spectrum shifts, since engine A centerline was 4.90 exit diameters above the ground, engine B centerline 3.20 diameters, and engine C centerline 4.4 diameters.

It is suggested by the work of Lighthill that subsonic air-jet power spectra fall on a single curve if the levels are corrected by the Lighthill relation (ordinate) and if Strouhal number rather than frequency is used as the abscissa.

Figure 21 shows the corrected power spectrum level as a function of Strouhal number for engine B at two thrust conditions. The corrected power spectrum level is defined as the power spectrum level corrected to a reference velocity V_r by 10 log $(V/V_r)^8$. The results of figure 21 show that for a particular engine the spectra over a range of thrust conditions can be fairly well correlated.

Comparison of air jets and engines.—A method of comparison of sound spectra which is independent of level, that is, jet velocity and area, is to plot cumulative sound power (fig. 17) as a function of Strouhal number. The results of such a plot for all three engines at rated power and for the 4-inch air jet at two pressure ratios are shown in figure 22. As might be expected, the air-jet data are in quite good agreement. The velocity V used in the Strouhal number was calculated for fully expanded flow for the case where the pressure ratio exceeded that for choking. The data at the higher pressure ratio indicate an increase in the higher frequency noise which results from the shock wave noise discussed previously (fig. 16).

The shapes of the curves for engines B and C differ considerably from the model jet data, as expected from the previous discussion (fig. 19) of reflection effects. The data for engine A (8 ft above ground) agree much better with the air-jet data and undoubtedly more nearly approach free-field spectra than the data for either engine B or C.

It would appear therefore that truly free-field data for either air jets or engines would peak at a Strouhal number of about 0.3.

Effect of nozzle shape of convergent nozzles with air jet.—Figure 23 shows the effect of nozzle shape on the sound spectra. All the nozzles considered in this figure had an exit area equivalent to the 4-inch-diameter circular nozzle. For all the data the shapes of the spectra are essentially independent of nozzle shape or position. This is particularly true at low pressure ratios and a 90° azimuth position (fig. 23 (c)), where the spread of the data is of the same order as the wind error. At the same position, but at a higher pressure ratio (fig. 23 (d)), all the data except the 4:1 elliptical nozzle in the vertical position are in good agreement. The data for the 4:1 ellipse in the vertical position show a tendency for a shift in energy to the higher frequencies for all the pressure ratios and positions. This shift to the higher frequencies is, as might be expected, due to the decreased effective nozzle dimension in the plane of the sound measurements.

Convergent-divergent and plug nozzles.—The sound spectra of the convergent-divergent nozzle for a wide range of pressure ratios are shown in figure 24. The large peak in the spectrum at 2500 cps and a pressure ratio of 2.27 disappears as the pressure ratio is increased to near the design value. The reduction in sound power (fig. 12) is due to the elimination of such noise.

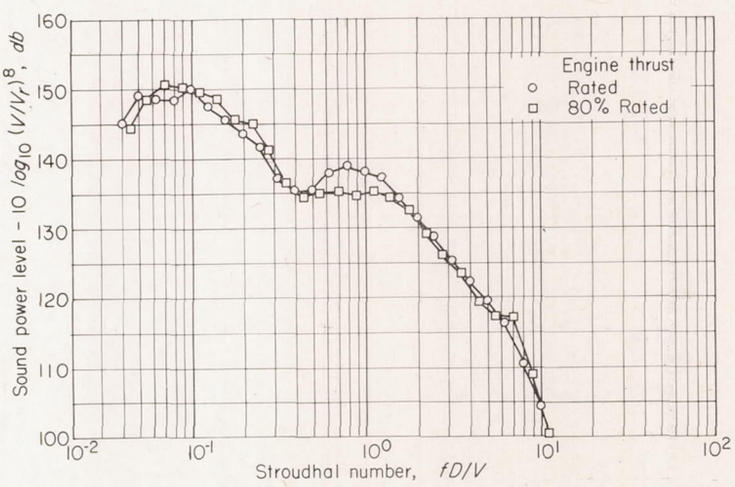

FIGURE 21.—Corrected spectrum power level as function of Strouhal number for engine B.

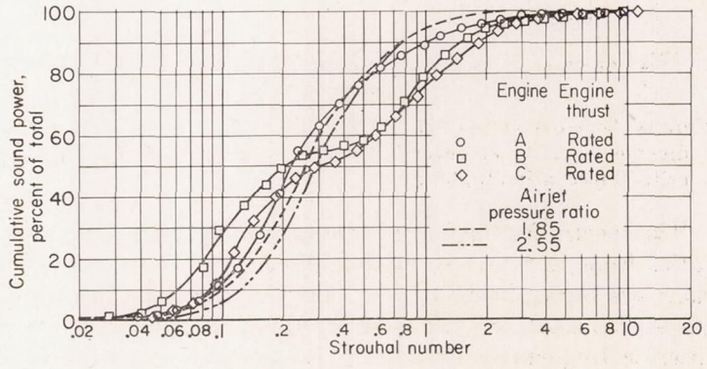

FIGURE 22.—Cumulative spectral distribution of sound power.

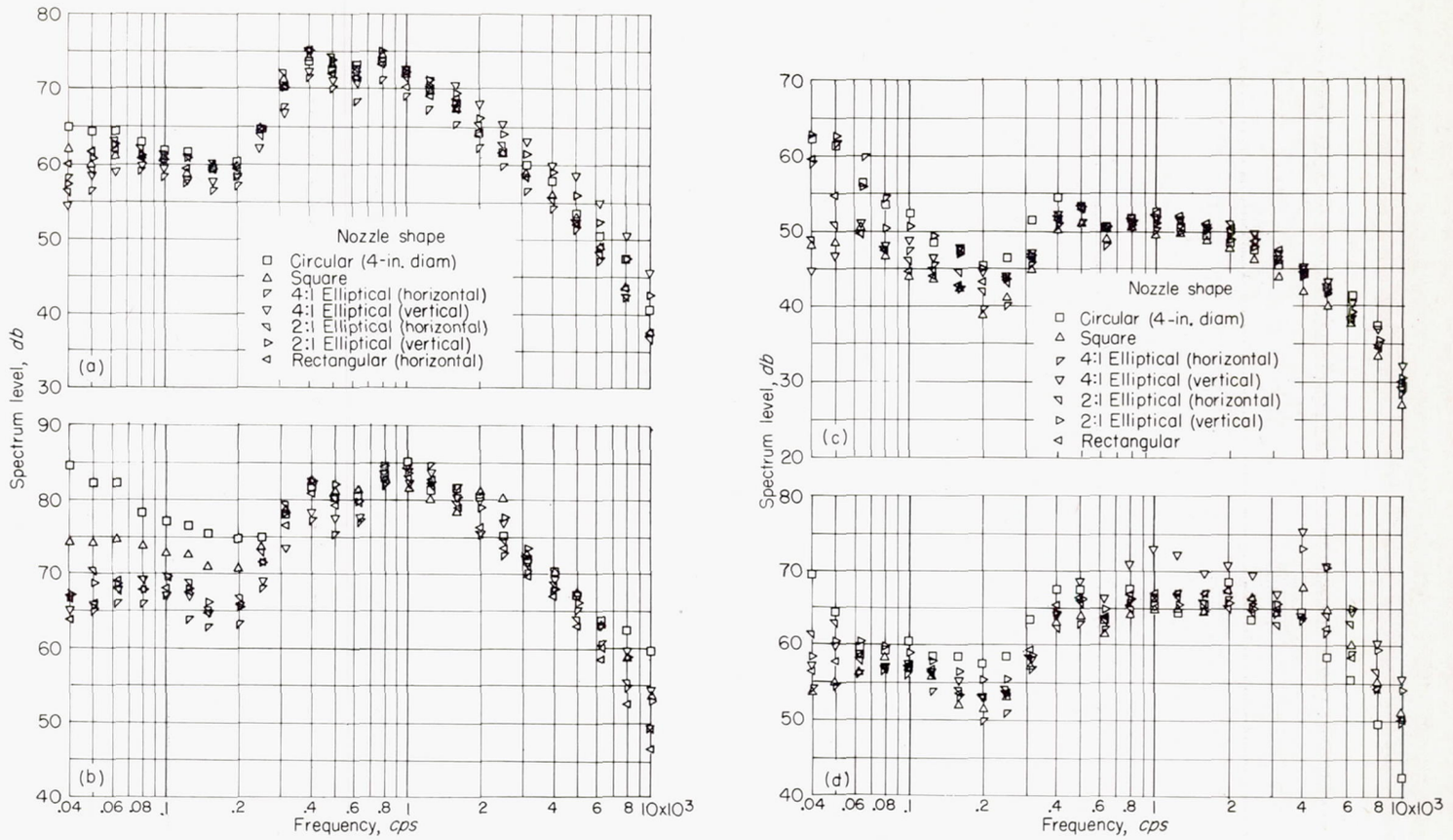

(a) Pressure ratio, 1.85; azimuth, 30°.
(b) Pressure ratio, 2.55; azimuth, 30°.
(c) Pressure ratio, 1.45; azimuth, 90°.
(d) Pressure ratio, 2.55; azimuth, 90°.

FIGURE 23.—Sound spectra for various convergent-nozzle shapes. Distance from jet exit, 50 feet.

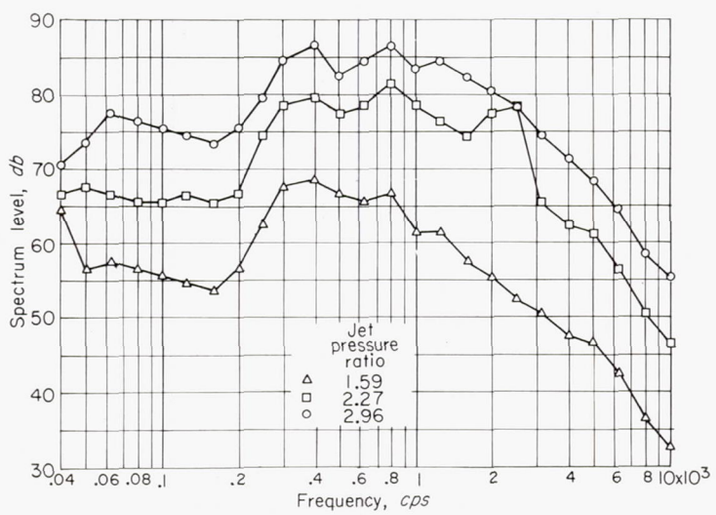

FIGURE 24.—Sound spectra of jet discharging from convergent-divergent nozzle at several pressure ratios. Distance from jet exit, 50 feet; azimuth, 30°.

The spectra for the four plug nozzles for a range of pressure ratios from 1.55 to 4.15 at the 30° and 90° azimuths (50-ft rad.) are shown in figure 25. The shapes of the spectra at the 90° azimuth are quite similar except for the existence of discrete frequencies at the highest pressure ratio. Strong peaks exist at 1200 and 2500 cps for the conical plug nozzle with a design pressure ratio of 4.0 (fig. 25(e)) and the isentropic plug nozzle with a design pressure ratio of 9.5 (fig. 25(h)). At the 30° position, the spectra are quite similar except for a single peak at a pressure ratio of 4.15 for the isentropic plug nozzle with a design pressure ratio of 9.5 (fig. 25(d)).

DIRECTIONAL EFFECTS

The directional characteristics of the noise are an important parameter in specifying the effect of a change in the sound generation. Conceivably, directional changes might be more significant in a particular case than changes in sound power or maximum sound level.

Circular convergent nozzles with air jet.—The effect of jet pressure ratio on the directional characteristics of a jet is illustrated by the sound polar diagram of figure 26. The results shown were obtained with the 4-inch-diameter circular convergent nozzle and are typical of those obtained with the various nozzle-exit diameters. At low pressure ratios, the maximum sound pressure level occurs about 30° from the jet axis, and the minimum occurs forward and 120° from the jet axis. At the high pressure ratios, the maximum still occurs at the 30° position, but a second peak occurs near the 90° position, and the minimum value at either 75° or 120°.

Figure 27 shows the directional characteristics of the noise (for three ⅓-octave frequency bands and the over-all frequency range) for the 4-inch-diameter air jet at two values of

jet pressure ratio. The directional distribution is symmetrical about the jet axis, and therefore only one side is presented. For frequency values up to and including 1000 cps, a pronounced lobe of higher sound-pressure level exists near the 30° azimuth from the jet direction. For frequencies above 1000 cps, the sound field is more nearly nondirectional. The over-all data (all frequencies) show the lobe at 30° with a relatively smooth, nearly circular pattern elsewhere.

Circular convergent nozzles with engines.—The complexity of the noise from a turbojet engine is illustrated by the directional distribution of the sound for engine B with no afterburning at 100- and 80-percent rated thrust (figs. 28(a) and (b), respectively) and with afterburning (fig. 28(c)). The prominent lobed regions centered between the 30° and 60° azimuths from the jet direction emphasize the

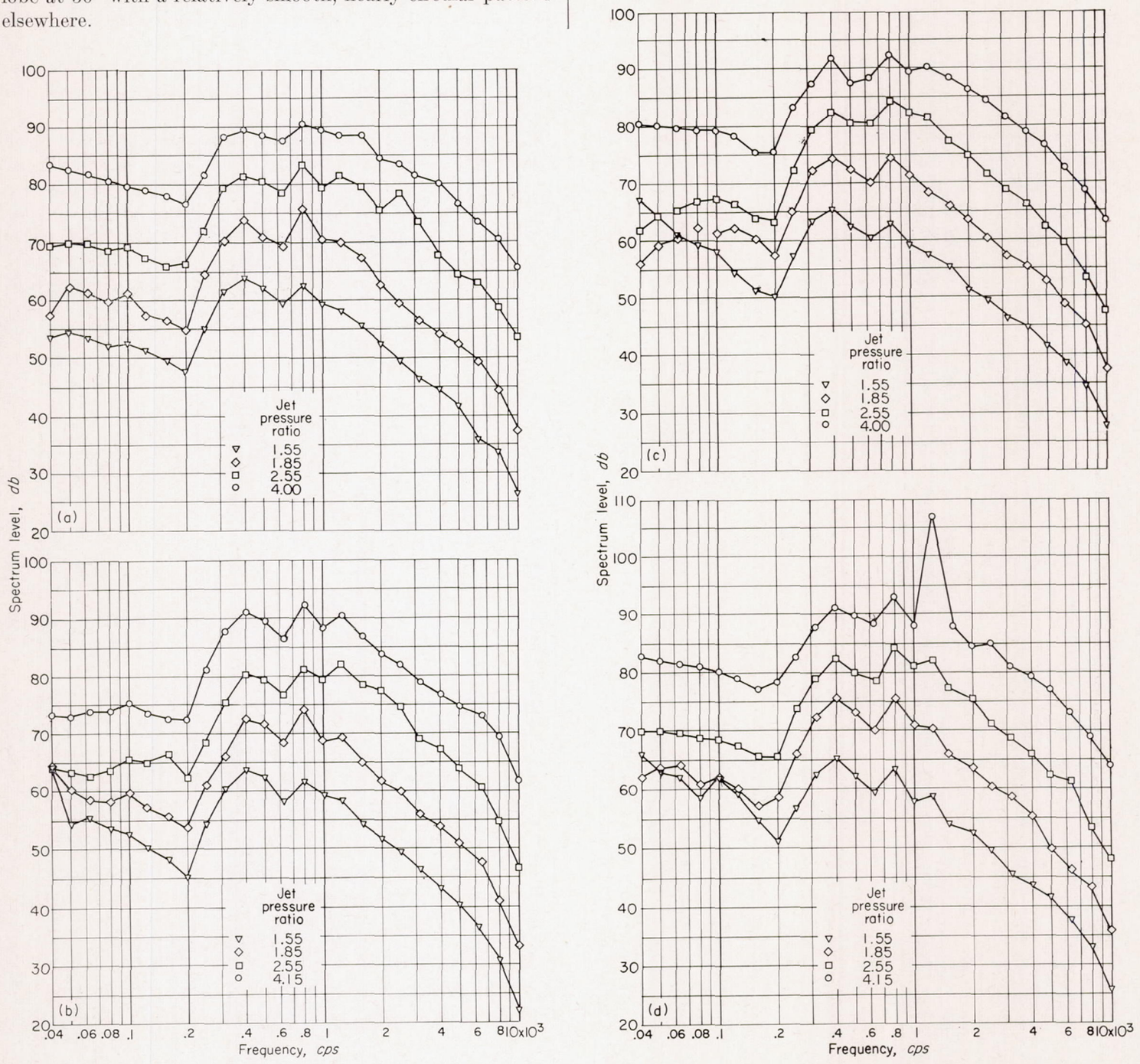

(a) Conical plug; design pressure ratio, 4.0; azimuth, 30°.
(b) Conical plug; design pressure ratio, 9.5; azimuth, 30°.
(c) Isentropic plug; design pressure ratio, 4.0; azimuth, 30°.
(d) Isentropic plug; design pressure ratio, 9.5; azimuth, 30°.

FIGURE 25.—Sound spectra of jet discharging from plug nozzle at several pressure ratios. Distance from jet exit, 50 feet.

considerable reduction in level at all frequencies in the direction directly behind the jet and to a 15° azimuth. In addition, relatively strong lobes are evident in the forward quadrant for many of the frequency bands. This is especially true of the 1000-cps data at rated engine thrust. This increase in the high-frequency noise forward of the engine is undoubtedly due to compressor noise.

Comparison of air jets and engines.—Polar diagrams of the corrected over-all directional distribution of the 4-inch-diameter air jet and two engines are shown in figure 29. The sound pressure levels have all been corrected to a reference value $(AV^8)_r$ by 10 log $AV^8/(AV^8)_r$. The comparison shows the sound patterns to be similar with the exception of the low-noise-level region displayed by both jet engines near the jet axis. This probably results from the refractive effect on the sound in passing from the jet to the surrounding atmosphere, in which the speed of sound is lower.

Effect of nozzle shape of convergent nozzles with air jet.—A comparison of the different nozzle-exit shapes at two pressure ratios is shown by the sound polar diagram of figure 30. At the low pressure ratio (fig. 30(a)) there is practically no effect of nozzle shape on the directional pattern, although the circular and square nozzles have slightly greater values than the other nozzles.

At the high pressure ratio (fig. 30(b)) there are no large differences in the sound polars. The circular nozzle has a slightly higher sound level than the other nozzle shapes. This is particularly evident 90° from the axis. As mentioned previously the slightly lower values obtained with the noncircular nozzle shapes may result from the asymmetry of the shock pattern. This asymmetry would reduce the discrete frequencies resulting from the regularity of the shock pattern as described in reference 2.

Convergent-divergent and plug nozzles.—The sound polar diagrams for the convergent-divergent nozzle for a range of pressure ratios are shown in figure 31. At the low pressure ratios the results are quite similar to those of the circular convergent nozzle (fig. 26). At the higher pressure ratios the convergent-divergent nozzle does not show the secondary peak at 90° and 270° exhibited by the ordinary circular con-

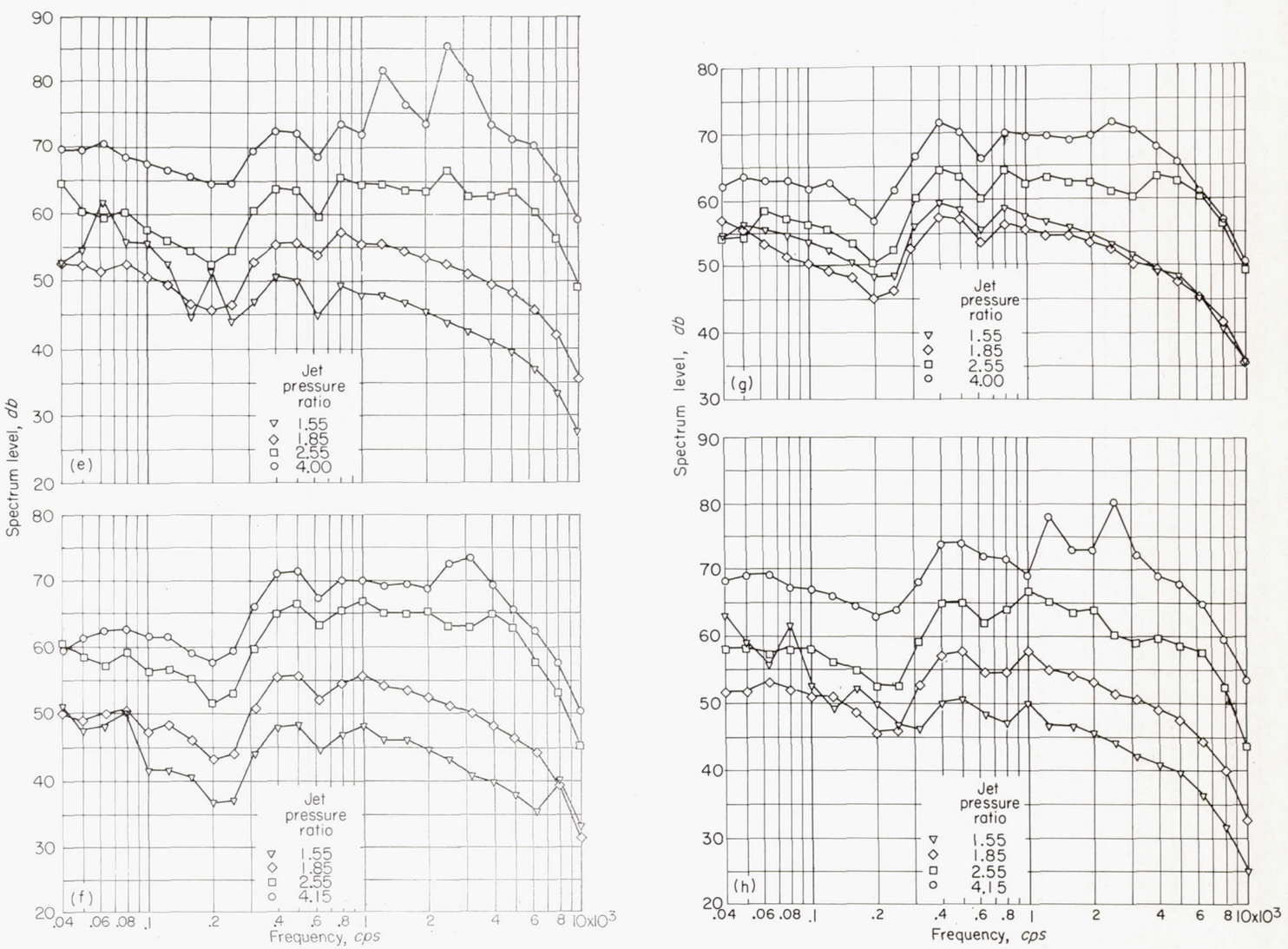

(e) Conical plug; design pressure ratio, 4.0; azimuth, 90°.
(f) Conical plug; design pressure ratio, 9.5; azimuth, 90°.
(g) Isentropic plug; design pressure ratio, 4.0; azimuth, 90°.
(h) Isentropic plug; design pressure ratio, 9.5; azimuth, 90°.

FIGURE 25.—Concluded. Sound spectra of jet discharging from plug nozzle at several pressure ratios. Distance from jet exit, 50 feet.

vergent nozzle (fig. 26). This effect, combined with slight changes over the entire sound field, results in reduced sound power as compared with a convergent nozzle.

The sound polar diagrams for all the plug nozzles for a range of pressure ratios are shown in figure 32. All these data are similar to the results obtained with the convergent nozzles. At both low and high pressure ratios the curves are similar in shape but at a slightly different level, which depends on the jet area.

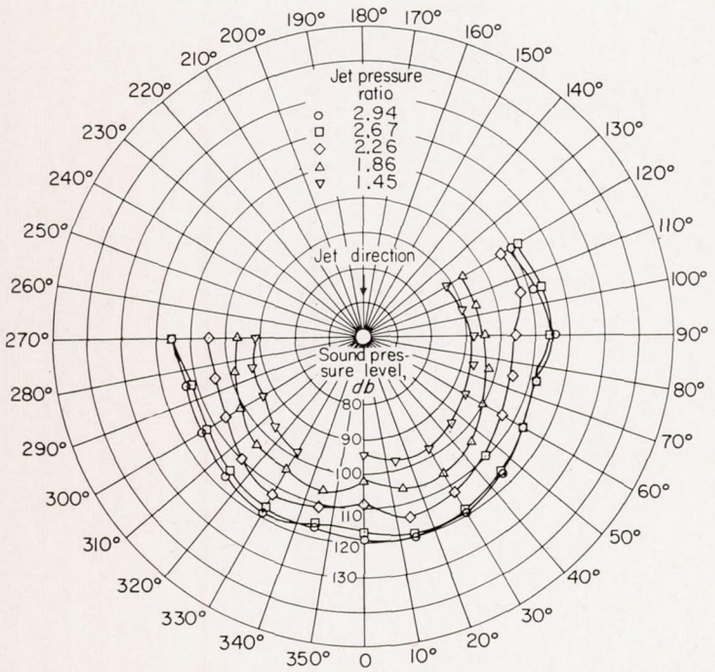

FIGURE 26.—Polar diagram of sound field for various pressure ratios of 4-inch-diameter circular convergent nozzle. Distance from jet exit, 50 feet.

SUMMARY OF RESULTS

As part of a general program to investigate jet noise and means for its suppression, a comparison was made of the noise characteristics of air jets and turbojet engines. The effect of nozzle shape on noise generation was studied with cold air jets. The following results were obtained:

1. At low jet pressure ratios (less than 2.2) the nozzle-exit shapes investigated had a negligible effect on the sound field (sound power, spectra, and direction) radiated by a jet.

2. The over-all sound power generated by an air jet or by a nonafterburning jet engine during ground operation at pressure ratios below or only slightly above that for choked flow was correlated by the Lighthill noise-generation parameter. This result shows that the principal contribution to jet-engine noise arose from the turbulent mixing of the jet with the surrounding atmosphere. The ratio of sound power to Lighthill parameter was found to be 2.7×10^{-5}.

3. The sound power radiated during afterburner operation of the engines was lower than indicated by the Lighthill parameter.

4. Correction of sound-pressure-level directional data by the nozzle-area ratio and $8th$ power of the velocity ratio gave good correlation of air-jet and engine data.

5. The spectral distribution of sound power for both air jets and engines was in good agreement for the case where the engine data were not greatly affected by reflection effects. For cases where the engine was located less than 4.9 diameters from the engine centerline to the ground, the reflection effects appear to cause a characteristic dip in the frequency spectrum at about 400 cps and a secondary peak at around 1000 cps.

6. Free-field power spectra (unaffected by reflection effects) for subsonic or a slightly choked engine or air jet show that the peak of the spectra occur at a Strouhal number of about 0.3.

7. At high jet pressure ratios the convergent nozzles of various exit shapes (circular, square, rectangular, and elliptical) all appeared to have essentially the same sound field. All these nozzles exhibited sound spectra having discrete-frequency-type noises due to shock waves.

8. At high jet pressure ratios considerable noise reduction was achieved by use of a convergent-divergent nozzle. The particular nozzle investigated produced one-third to one-half as much sound power as a convergent nozzle at a pressure ratio near 2.9. This reduction in sound power resulted from the elimination of discrete frequencies due to shock waves.

9. The series of plug nozzles (designed for high jet pressure ratios) investigated did not show the reduction in sound power or discrete frequencies obtained with the convergent-divergent nozzle. These nozzles showed characteristics similar to convergent nozzles over a range of jet pressure ratios from 1.45 to 4.2.

LEWIS FLIGHT PROPULSION LABORATORY
NATIONAL ADVISORY COMMITTEE FOR AERONAUTICS
CLEVELAND, OHIO, *MARCH 19, 1957*

REFERENCES

1. Westley, R., and Lilley, G. M.: An Investigation of the Noise Field from a Small Jet and Methods for Its Reduction. Rep. No. 53, The College of Aero. (Cranfield), Jan. 1952.
2. Powell, A.: On the Mechanism of Choked Jet Noise. Proc. Phys. Soc., sec. B., vol. 66, pt. 12, no. 408B, Dec. 1953, pp. 1039–1056.
3. Lighthill, M. J.: On Sound Generated Aerodynamically. I—General Theory. Proc. Roy. Soc. (London), ser. A., vol. 211, no. 1107, Mar. 20, 1952, pp. 564–587.
4. Tyler, John M., and Perry, Edward C.: Jet Noise. Preprint No. 287, SAE, 1954.
5. Lee, Robert: Free Field Measurements of Sound Radiated by Subonic Air Jets. Rep. 868, Navy Dept., The David W. Taylor Model Basin, Dec. 1953.
6. Bolt, R. H., Lukasik, S. J., Nolle, A. W., and Frost, A. D., eds.: Handbook of Acoustic Noise Control. Vol. I. Physical Acoustics. WADC Tech. Rep. 52–204, Aero. Medical Lab. Wright Air Dev. Center, Wright-Patterson Air Force Base, Dec. 1952. (Contract No. AF 33(038)–20572, RDO No. 695–63.)
7. Callaghan, Edmund E., and Coles, Willard D.: Investigation of Jet-Engine Noise Reduction by Screens Located Transversely Across the Jet. NACA TN 3452, 1955.
8. Lassiter, Leslie W., and Hubbard, Harvey H.: The Near Noise Field of Static Jets and Some Model Studies of Devices for Noise Reduction. NACA Rep. 1261, 1956. (Supersedes NACA TN 3187.)
9. Fay, R. C.: Plane Sound Waves of Finite Amplitude. Jour. Acous. Soc. Am., vol. 3, Oct. 1931, pp. 222–241.
10. Franken, Peter A.: The Field of a Random Noise Source Above an Infinite Plane. Theoretical Analysis. Acoustics Lab., M. I. T., Jan. 11, 1955.

438639—58——3

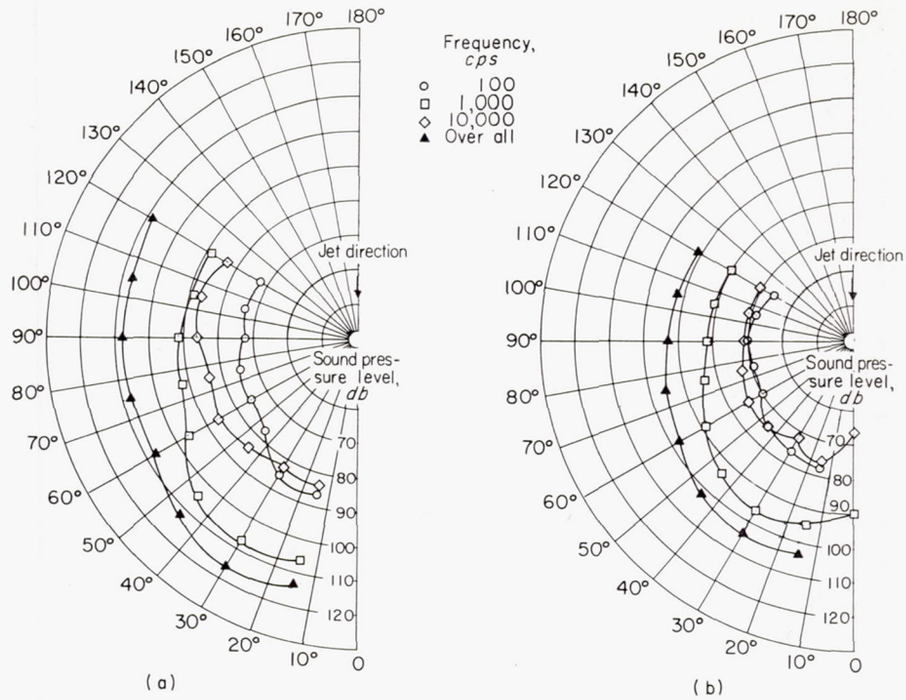

(a) Jet pressure ratio, 2.55. (b) Jet pressure ratio, 1.86.

FIGURE 27.—Directional distribution of noise from 4-inch-diameter air jet. Distance from jet exit, 50 feet.

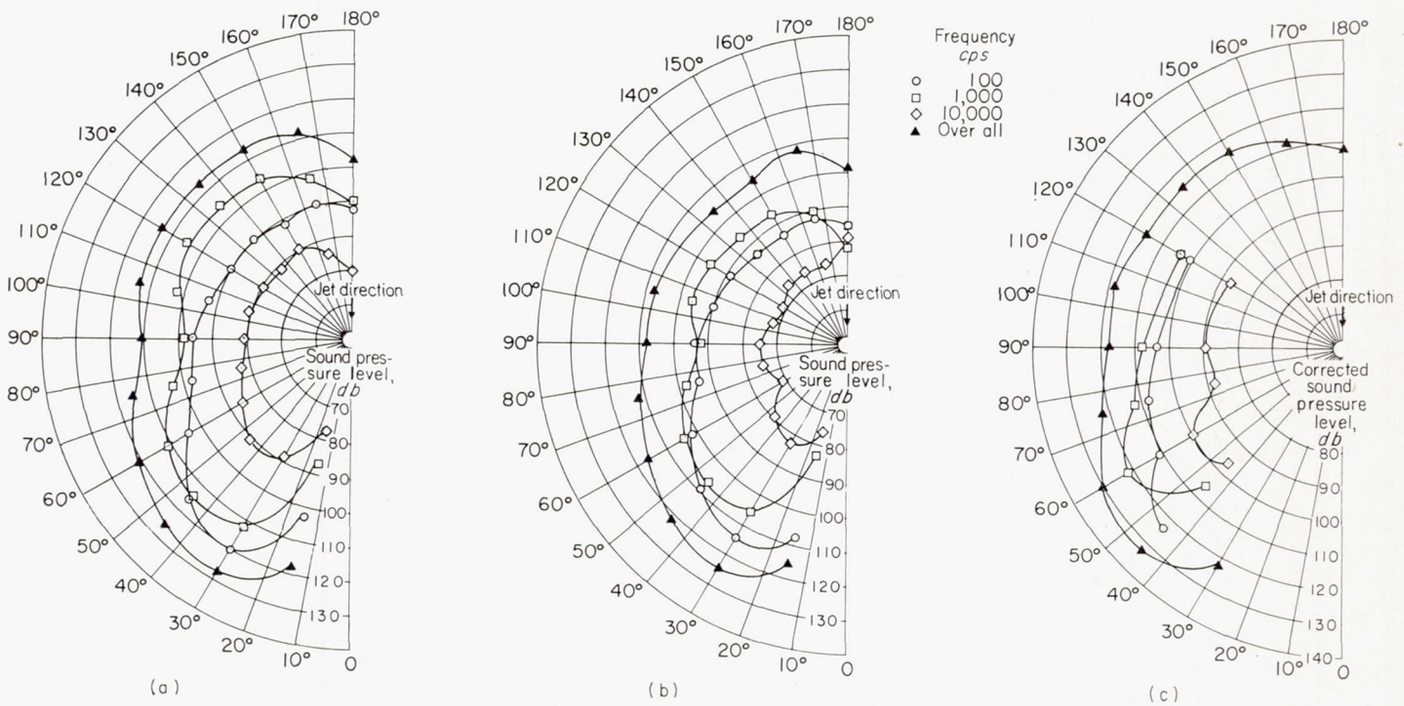

(a) 100 percent thrust; no afterburning. (b) 80 percent thrust; no afterburning. (c) Afterburning; distance corrected to 200 feet.

FIGURE 28.—Directional distribution of noise from engine B. Distance from jet exit, 200 feet.

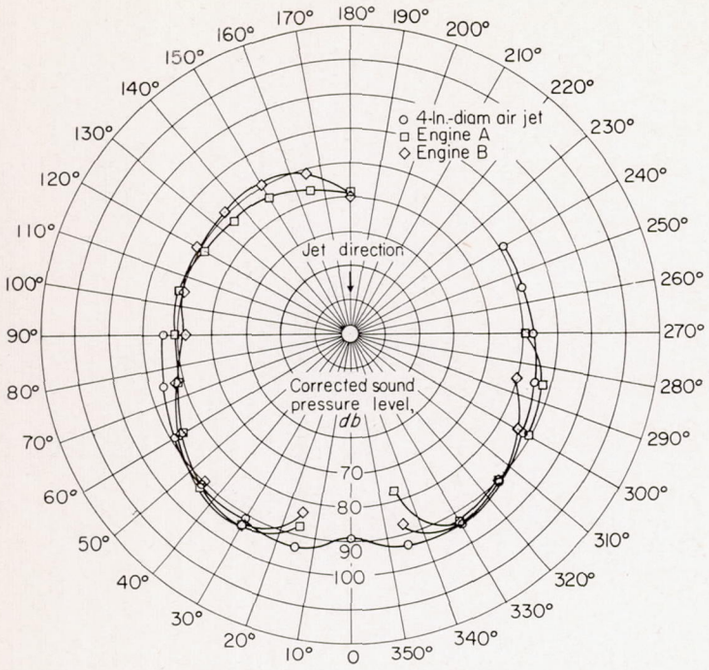

FIGURE 29.—Comparison of directional distribution of sound from air jet and engines. Area-ratio corrections and velocity-ratio corrections to the 8*th* power based on an air jet have been applied. Distance from jet exit, corrected to 200 feet.

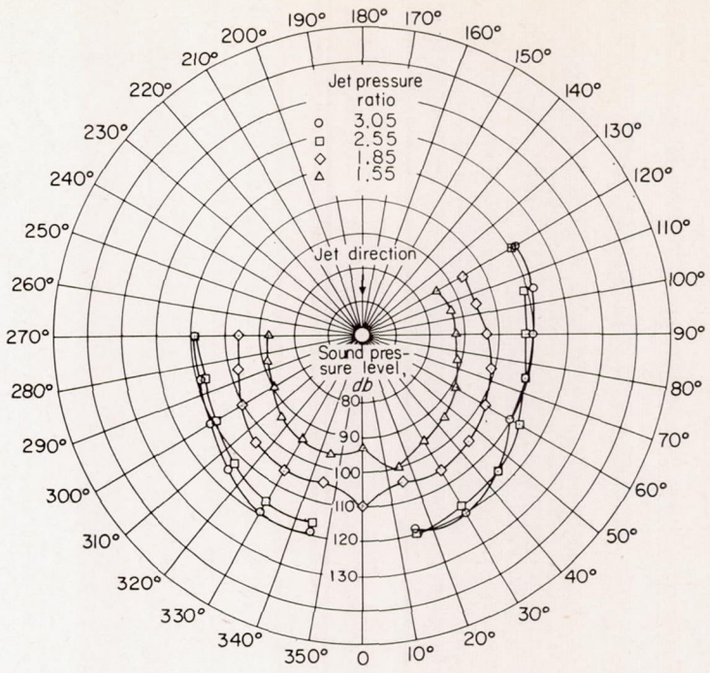

FIGURE 31.—Sound polar diagram of 4-inch-diameter convergent-divergent nozzle for range of pressure ratios. Distance from jet exit, 50 feet.

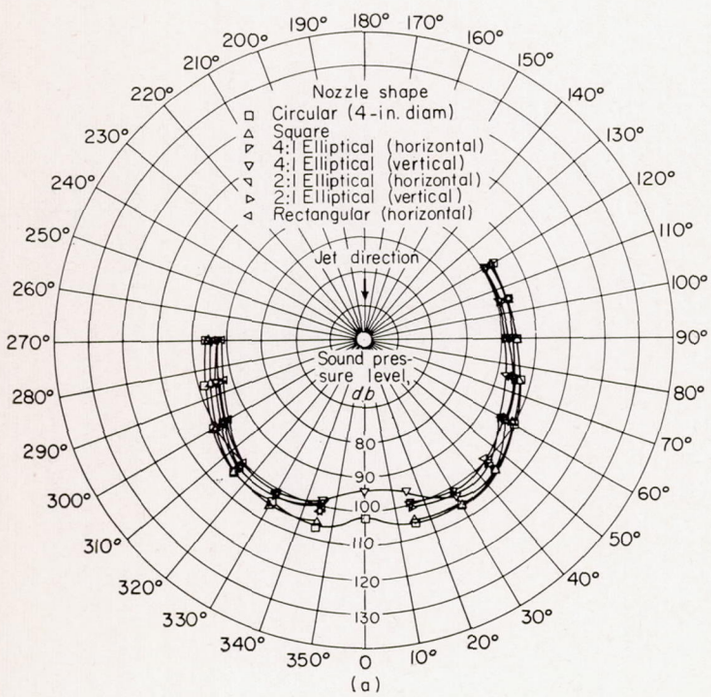

(a) Jet pressure ratio, 1.85.

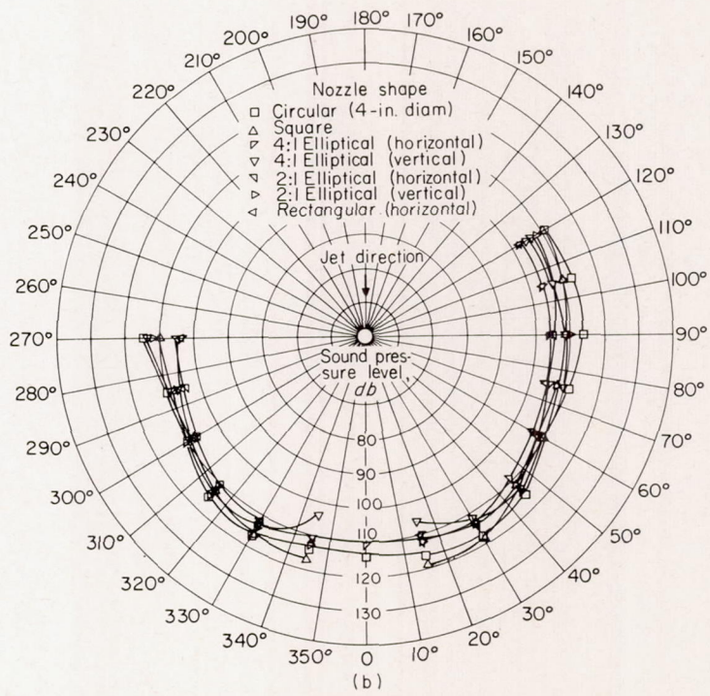

(b) Jet pressure ratio, 2.55.

FIGURE 30.—Effect of nozzle shape on sound-field direction. Distance from jet exit, 50 feet.

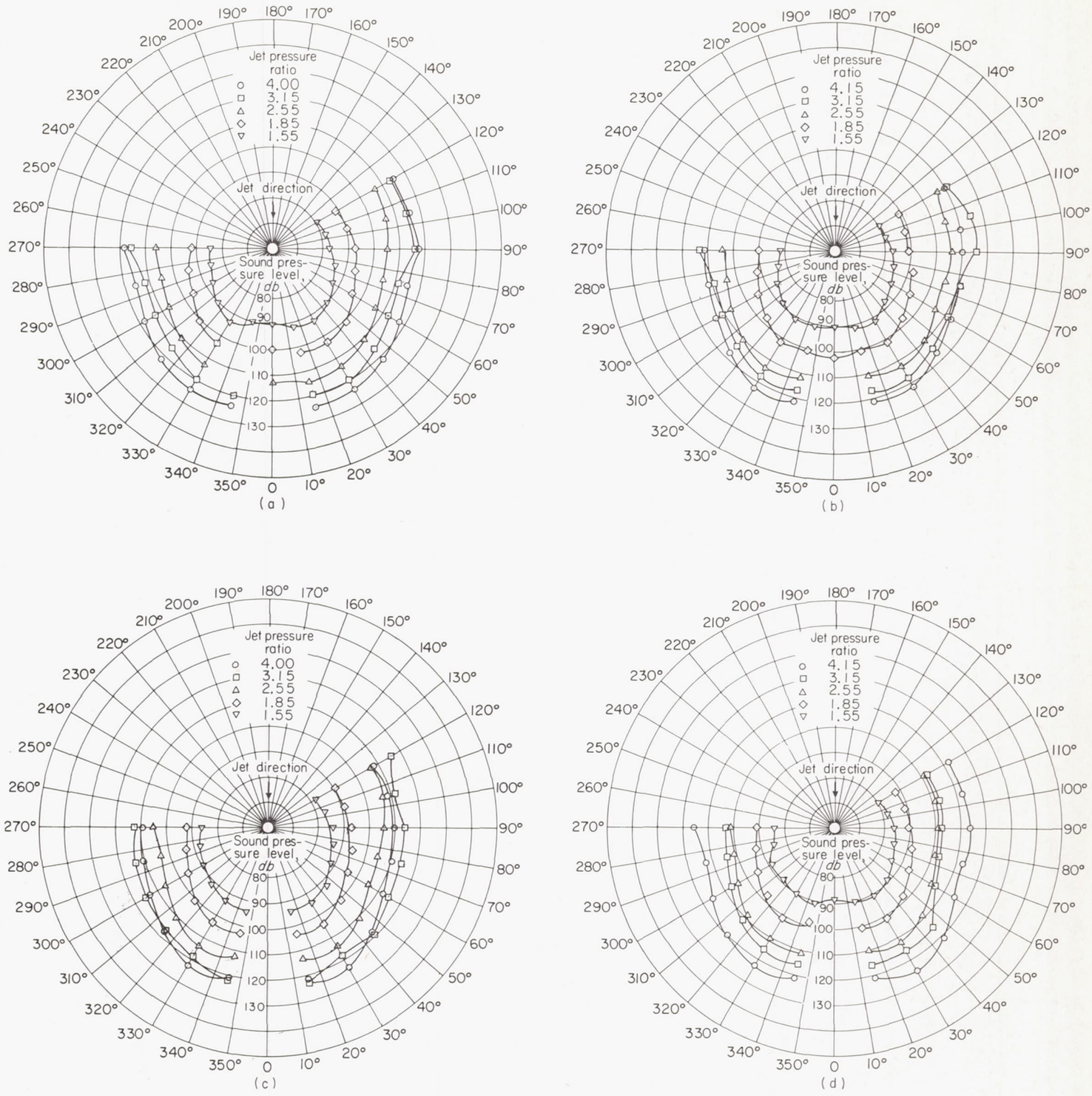

(a) Conical plug; design pressure ratio, 4.0.
(b) Conical plug; design pressure ratio, 9.5.
(c) Isentropic plug; design pressure ratio, 4.0.
(d) Isentropic plug; design pressure ratio, 9.5.

FIGURE 32.—Polar diagram of sound field for plug nozzles at various pressure ratios. Distance from jet exit, 50 feet.

U. S. GOVERNMENT PRINTING OFFICE: 1958